Harmonic and subharmonic association of universal dimers in a thermal gas

Abhishek Mohapatra and Eric Braaten

Phys. Rev. A **92**, 013425 — Published 28 July 2015

DOI: 10.1103/PhysRevA.92.013425

Harmonic and Subharmonic Association of Universal Dimers in a Thermal Gas

Abhishek Mohapatra* and Eric Braaten†

Department of Physics,
The Ohio State University,
Columbus, OH 43210, USA

Abstract

In a gas of ultracold atoms whose scattering length is controlled by a magnetic Feshbach resonance, atoms can be associated into universal dimers by an oscillating longitudinal magnetic field. In addition to the harmonic resonance with frequency near that determined by the dimer binding energy, there is a subharmonic resonance with half that frequency. If the thermal gas contains dimers, they can be dissociated into unbound atoms by the oscillating magnetic field. We show that the transition rates for association and dissociation can be calculated by treating the oscillating magnetic field as a sinusoidal time-dependent perturbation proportional to the contact operator. Many-body effects are taken into account through transition matrix elements of the contact operator. We calculate both the harmonic and subharmonic transition rates analytically for association in a thermal gas of atoms and for dissociation in a thermal gas of dimers.

PACS numbers: 31.15.-p, 34.50.-s, 67.85.Lm, 03.75.Nt, 03.75.Ss
Keywords: Fermi gases, scattering of atoms and molecules.

*Electronic address: mohapatra.16@buckeyemail.osu.edu
†Electronic address: braaten@mps.ohio-state.edu

I. INTRODUCTION

The use of *magnetic Feshbach resonances* to control the interaction strengths of ultracold atoms has led to significant advances in our understanding of strong interactions in few-body and many-body physics. The effects of time-dependent strong interactions can be studied by using a time-dependent *longitudinal* magnetic field. A particularly interesting case is a *sinusoidal* modulation. Atoms can be associated into universal molecules composed of atoms with a large scattering length by modulating the magnetic field with a frequency near the binding frequency of the molecule. The measurement of the binding energy of a molecule by observing a loss resonance near the binding frequency is called *magnetic-field modulation spectroscopy* or sometimes *wiggle spectroscopy*.

The association of atoms into dimers by the longitudinal modulation of the magnetic field was pioneered by Thompson, Hodby, and Wieman, who used it to associate ^{85}Rb atoms into dimers [1]. Greiner, Regal, and Jin used magnetic-field modulation to dissociate paired fermions and excite a collective mode in a gas of ^{40}K atoms in the BCS-BEC crossover region [2]. Papp and Wieman used magnetic-field modulation spectroscopy to measure the binding energies of dimers composed of ^{85}Rb and ^{87}Rb atoms [3]. Weber et al. used a modulated magnetic field to associate ^{41}K and ^{87}Rb atoms into dimers and to measure their binding energies [4]. They also observed subharmonic resonances near half the binding frequency of the dimer. Lange et al. used magnetic-field modulation spectroscopy to measure the binding energies of ^{133}Cs dimers [5]. Pollack et al. used a modulated magnetic field to excite collective modes in a Bose-Einstein condensate of ^{7}Li atoms [6]. Gross et al. and Machtey et al. used a modulated magnetic field to associate ^{7}Li atoms into dimers [7, 8] and into Efimov trimers [9]. Dyke, Pollack, and Hulet used magnetic-field modulation spectroscopy to measure the binding energies of ^{7}Li dimers in both a Bose-Einstein condensate and a thermal gas [10]. In the thermal gas, they also observed a subharmonic resonance. Smith recently pointed out that a sinusoidally oscillating magnetic field near a Feshbach resonance can be used to control the scattering length, and he showed that the resonance parameters are universal functions of the magnetic field [11].

A theoretical treatment of the association of atoms into dimers by an oscillating longitudinal magnetic field was first presented by Hanna, Köhler, and Burnett in 2007 [12]. They described the two-atom system by a two-channel model consisting of a continuum of atom-pair states and a discrete molecular state. They calculated the probability for the association of atom pairs into dimers as a function of time by solving the time-dependent Schrödinger equation for the two coupled channels. Their results for the association probabilities were completely numerical. Brouard and Plata simplified the problem to a two-state model consisting of an atom-pair state and a molecular state [13]. They deduced some qualitative aspects of the harmonic and subharmonic association processes from an analytic approximation to the two-state problem. Bazak, Liverts and Barnea considered the association of atoms into dimers by a modulated magnetic field whose oscillatory component is in an arbitrary direction [14]. They used first-order time dependent perturbation theory and Fermi's Golden Rule to obtain an analytic result for the association rate as a function of the oscillation frequency. Their result vanishes if the oscillatory component of the magnetic field is longitudinal.

A much simpler approach to this problem was recently introduced in Ref. [15]. It was inspired by Tan's *adiabatic relation*, which expresses the change in the energy E of a system due to a change in the scattering length a in terms of an extensive thermodynamic variable

that is conjugate to $1/a$ called the *contact* C [16]. In the case of fermions with mass m and two spin states, the adiabatic relation is

$$\frac{d}{d(1/a)}E = -\frac{\hbar^2}{4\pi m}C. \tag{1}$$

(In the case of identical bosons, the right side should be multiplied by 1/2.) Ref. [15] pointed out that the transition rates for the association of atoms into universal dimers can be calculated by treating the oscillating longitudinal magnetic field as a sinusoidal time-dependent perturbation proportional to the contact operator. The association rates were calculated for a thermal gas of atoms and for a dilute Bose-Einstein condensate of atoms. In this approach, many-body effects are taken into account through transition matrix elements of the contact operator.

In this paper, we extend the approach of Ref. [15] to subharmonic transitions and to the dissociation rates of universal dimers. In Sections II, we derive general formulas for the harmonic and subharmonic transition rates using time-dependent perturbation theory. In Sections III and IV, we calculate the leading harmonic contributions to the association rate in a thermal gas of atoms and the dissociation rate in a thermal gas of dimers. They come from a first-order perturbation in the contact operator. In Sections V and VI, we calculate the dominant subharmonic contributions to the association rate in a thermal gas of atoms and the dissociation rate in a thermal gas of dimers. They come from a second-order perturbation in the contact operator. In Section VII, we describe briefly previous experiments on association using longitudinal modulation of the magnetic field. In Section VIII, we describe briefly previous theoretical treatments of association into dimers using longitudinal modulation of the magnetic field. We summarize our results in Section IX.

II. TRANSITION RATES

In this section, we derive general formulas for transition rates at first order and second order in time-dependent perturbation theory. We focus on the case of fermionic atoms with equal mass m and two spin states. (We also give the corresponding results for identical bosons.)

A. Perturbing Hamiltonians

Near a magnetic Feshbach resonance, the scattering length a of the atoms is a function of the magnetic field:

$$a(B) = a_{\rm bg}[1 - \Delta/(B - B_0)], \tag{2}$$

where $a_{\rm bg}$ is the background scattering length and B_0 and $B_0+\Delta$ are the positions of the pole and the zero of the scattering length, respectively. We consider a time-dependent magnetic field with a fixed direction $\hat{\boldsymbol{z}}$. Its magnitude has a constant bias value $\bar{B}$ for $t < 0$, and it is modulated with a small amplitude b around that bias value for $t > 0$:

$$\boldsymbol{B}(t) = \bar{B}\hat{\boldsymbol{z}} \qquad t < 0, \tag{3a}$$

$$= \left[\bar{B} + b\sin(\omega t)\right]\hat{\boldsymbol{z}} \qquad t > 0. \tag{3b}$$

If the magnetic field B in Eq. (2) is replaced by the oscillating field $\bar{B} + b\sin(\omega t)$, it implies a time-dependent scattering length $a(t)$.

Tan's adiabatic relation in Eq. (1) implies that the leading perturbation in the Hamiltonian for $t > 0$ is proportional to the contact operator:

$$H(t) - H(0) = -\frac{\hbar^2}{4\pi m}\left(\frac{1}{a(t)} - \frac{1}{\bar{a}}\right) C, \tag{4}$$

where $\bar{a} = a(\bar{B})$ is the scattering length for the bias magnetic field. In Appendix A, quantum field theory methods are used to argue that this is the only perturbation that contributes in the zero-range limit. The inverse scattering length can be expanded in powers of b:

$$\frac{1}{a(t)} = \frac{1}{\bar{a}} - \frac{1}{a_{\rm bg}}\left(\frac{b\Delta}{(\Delta + B_0 - \bar{B})^2}\right)\sin(\omega t) - \frac{1}{a_{\rm bg}}\left(\frac{b^2\Delta}{(\Delta + B_0 - \bar{B})^3}\right)\sin^2(\omega t) + \ldots. \tag{5}$$

The coefficients of the powers of b have well-behaved limits as $\bar{B}$ approaches the Feshbach resonance at B_0. Inserting the expansion in Eq. (5) into Eq. (4), we can identify terms in the perturbing Hamiltonian that are first and second order in b:

$$H_1(t) = \frac{\hbar^2}{4\pi m a_{\rm bg}}\left(\frac{b\Delta}{(\Delta + B_0 - \bar{B})^2}\right) C\sin(\omega t), \tag{6a}$$

$$H_2(t) = \frac{\hbar^2}{4\pi m a_{\rm bg}}\left(\frac{b^2\Delta}{(\Delta + B_0 - \bar{B})^3}\right) C\sin^2(\omega t). \tag{6b}$$

(In the case of identical bosons, the right sides should be multiplied by 1/2.) If $|b| \ll |\Delta|$, the effects of H_1 and H_2 can be taken into account as time-dependent perturbations. The first-order perturbation in H_1 drives transitions to states whose energies are higher or lower by $\hbar\omega$. We refer to such transitions as *harmonic* transitions. The first-order perturbation in H_2 and the second-order perturbation in H_1 both drive transitions to states whose energies differ by 0 or $\pm 2\hbar\omega$. We refer to transitions to states whose energies are higher or lower by $2\hbar\omega$ as *subharmonic* transitions.

B. Fermi's Golden Rule

We first consider transitions from the first-order perturbation in H_1. We take the initial state $|i\rangle$ to be an energy eigenstate with energy E_i. We consider the transition to a distinct energy eigenstate $|f\rangle$ with energy E_f. At first order in perturbation theory, the probability amplitude for the final state $|f\rangle$ at time T is

$$a_f^{(1)}(T) = \frac{i\hbar}{8\pi m a_{\rm bg}}\left(\frac{b\Delta}{(\Delta + B_0 - \bar{B})^2}\right)\left[\frac{e^{i(\omega_{fi}+\omega)T} - 1}{\omega_{fi} + \omega} - \frac{e^{i(\omega_{fi}-\omega)T} - 1}{\omega_{fi} - \omega}\right]\langle f|C|i\rangle, \tag{7}$$

where $\omega_{fi} = (E_f - E_i)/\hbar$. The two terms inside the brackets have absolute values that increase linearly with T in the limits $\omega_{fi} \to -\omega$ and $\omega_{fi} \to +\omega$, respectively. By applying Fermi's Golden Rule, we obtain the transition rate summed over final states $|f\rangle$:

$$\Gamma_1^{(1)}(\omega) = \frac{\hbar^2}{64\pi^2 m^2 a_{\rm bg}^2}\left(\frac{b\Delta}{(\Delta + B_0 - \bar{B})^2}\right)^2 \sum_f \left|\langle f|C|i\rangle\right|^2 \sum_{\pm} 2\pi\delta(\omega_{fi} \pm \omega). \tag{8}$$

(In the case of identical bosons, the prefactor should be multiplied by 1/4.) This transition rate is non-zero only for final states whose energy differs from E_i by $\pm\hbar\omega$, so it contributes to the harmonic transition rate $\Gamma_1(\omega)$. The superscript (1) on $\Gamma_1^{(1)}$ indicates that it comes from the first-order perturbation in H_1.

We next consider transitions from the first-order perturbation in H_2. At first order in perturbation theory, the probability amplitude for the final state $|f\rangle$ at time T is

$$a_f^{(2)}(T) = \frac{\hbar}{16\pi m a_{\rm bg}} \left(\frac{b^2\Delta}{(\Delta + B_0 - \bar{B})^3}\right) \left[\frac{e^{i(\omega_{fi}+2\omega)T}-1}{\omega_{fi}+2\omega} + \frac{e^{i(\omega_{fi}-2\omega)T}-1}{\omega_{fi}-2\omega} + \ldots\right] \langle f|C|i\rangle. \tag{9}$$

Inside the brackets, we have shown explicitly only those terms whose absolute values increase linearly with T in the limits $\omega_{fi} \to \pm 2\omega$. By applying Fermi's Golden Rule, we obtain the transition rate summed over final states $|f\rangle$:

$$\Gamma_2^{(2)}(\omega) = \frac{\hbar^2}{256\pi^2 m^2 a_{\rm bg}^2} \left(\frac{b^2\Delta}{(\Delta + B_0 - \bar{B})^3}\right)^2 \sum_f \left|\langle f|C|i\rangle\right|^2 \sum_{\pm} 2\pi\delta(\omega_{fi} \pm 2\omega). \tag{10}$$

(In the case of identical bosons, the prefactor should be multiplied by 1/4.) This transition rate is nonzero only for final states whose energy differs from E_i by $\pm 2\hbar\omega$, so it contributes to the subharmonic transition rate $\Gamma_2(\omega)$. The superscript (2) on $\Gamma_2^{(2)}$ indicates that it comes from the first-order perturbation in H_2. The subharmonic transition rate in Eq. (10) is determined by the same transition matrix element $\langle f|C|i\rangle$ of the contact operator as the harmonic transition rate in Eq. (8). It can be expressed in terms of the leading harmonic transition rate at twice the frequency:

$$\Gamma_2^{(2)}(\omega) = \frac{1}{4}\left(\frac{b}{\Delta + B_0 - \bar{B}}\right)^2 \Gamma_1^{(1)}(2\omega). \tag{11}$$

Finally we consider transitions from the second-order perturbation in H_1. At second order in perturbation theory, the probability amplitude for the final state $|f\rangle$ at time T is

$$\begin{aligned} a_f^{(1,1)}(T) \;=\; -\frac{\hbar^2}{64\pi^2 m^2 a_{\rm bg}^2} \left(\frac{b\Delta}{(\Delta + B_0 - \bar{B})^2}\right)^2 \sum_m \langle f|C|m\rangle\langle m|C|i\rangle \\ \times \left[\frac{e^{i(\omega_{fi}+2\omega)T}-1}{(\omega_{fi}+2\omega)(\omega_{mi}+\omega)} + \frac{e^{i(\omega_{fi}-2\omega)T}-1}{(\omega_{fi}-2\omega)(\omega_{mi}-\omega)} + \ldots\right], \end{aligned} \tag{12}$$

where the sum is over intermediate states $|m\rangle$. Inside the brackets, we have shown explicitly only those terms whose absolute values increase linearly with T if ω_{fi} is $\pm 2\omega$. By applying Fermi's Golden Rule, we obtain the transition rate summed over final states $|f\rangle$:

$$\Gamma_2^{(1,1)}(\omega) = \frac{\hbar^4}{4096\pi^4 m^4 a_{\rm bg}^4} \left(\frac{b\Delta}{(\Delta + B_0 - \bar{B})^2}\right)^4 \sum_f \sum_{\pm} \left|\sum_m \frac{\langle f|C|m\rangle\langle m|C|i\rangle}{\omega_{mi} \pm \omega}\right|^2 2\pi\delta(\omega_{fi} \pm 2\omega). \tag{13}$$

(In the case of identical bosons, the prefactor should be multiplied by 1/16.) This transition rate is nonzero only for final states whose energy differs from E_i by $\pm 2\hbar\omega$, so it contributes to the subharmonic transition rate $\Gamma_2(\omega)$. The superscript (1,1) on $\Gamma_2^{(1,1)}$ indicates that it

comes from the second-order perturbation in H_1. There is an additional factor of $1/a_{\rm bg}^2$ in the prefactor for $\Gamma_2^{(1,1)}$ compared to $\Gamma_2^{(2)}$. The relative importance of these two contributions is determined by the canceling length scales provided by the contact matrix elements and the frequency denominator. If $\Gamma_2^{(1,1)}$ and $\Gamma_2^{(2)}$ have the same order of magnitude, the interference between the first-order perturbation in H_2 and the second-order perturbation in H_1 would have to be taken into account. By explicit calculations of subharmonic transition rates in a thermal gas, we will find that the additional dimensionless factor in $\Gamma_2^{(1,1)}$ is $(\bar{a}/a_{\rm bg})^2$. Thus $\Gamma_2^{(1,1)}$ is much larger than $\Gamma_2^{(2)}$ if $\bar{B}$ is near a Feshbach resonance.

C. Thermal System

The transitions rates in Eqs. (8), (10), and (13) apply to an initial state $|i\rangle$ that is an energy eigenstate. A thermal system is described instead by a density matrix. For a completely thermalized system, the density matrix is $\rho = \exp(-\beta H)/\mathrm{Tr}(\exp(-\beta H))$, where H is the Hamiltonian and $\beta = 1/k_B T$. By expressing the modulus-squared of an amplitude as the product of the amplitude and its complex conjugate, the dependence on the initial state in Eqs. (8), (10), and (13) can be put in the form of the projection operator $|i\rangle\langle i|$ multiplied by a function $F(E_i)$ of the initial energy that includes the frequency delta function. If the density matrix ρ is diagonal in an energy basis, the transition rate is obtained by making the substitution

$$F(E_i)\,|i\rangle\langle i| \longrightarrow \sum_i F(E_i)\,|i\rangle\langle i|\rho|i\rangle\langle i|. \tag{14}$$

D. Homogeneous System

The contact operator C is an extensive variable. It can be expressed as the integral over space of the *contact density* operator:

$$C = \int d^3r\, \mathcal{C}(\boldsymbol{r}). \tag{15}$$

If the initial and final states are homogeneous systems, we can simplify the transition rates by expressing them in terms of matrix elements of the contact density operator.

The harmonic transition rate $\Gamma_1^{(1)}(\omega)$ in Eq. (8) and the subharmonic transition rate $\Gamma_2^{(2)}(\omega)$ in Eq. (10) involve the factor $|\langle f|C|i\rangle|^2$. By inserting the expression for C in Eq. (15), we obtain matrix elements of the contact density at two different positions. We can use translational invariance to put both operators at the same position $\boldsymbol{r}$. One of the integrals over space then gives a momentum-conserving delta function. The resulting expression for the modulus-squared of the transition matrix element is

$$\sum_f \left|\langle f|C|i\rangle\right|^2 = \sum_f (2\pi)^3 \delta^3(\boldsymbol{K}_f - \boldsymbol{K}_i) \int d^3r \left|\langle f|\mathcal{C}(\boldsymbol{r})|i\rangle\right|^2, \tag{16}$$

where $\boldsymbol{K}_i$ and $\boldsymbol{K}_f$ are the total wave vectors of the initial and final states of the homogeneous system, respectively. Homogeneity implies that $\left|\langle f|\mathcal{C}(\boldsymbol{r})|i\rangle\right|^2$ is independent of the position $\boldsymbol{r}$. Thus the integral $\int d^3r$ in Eq. (16) just gives a factor of the volume V.

The subharmonic transition rate $\Gamma_2^{(1,1)}(\omega)$ in Eq. (13) involves the product of four matrix elements of C. By inserting the expression for C in Eq. (15), we obtain matrix elements of the contact density at four different positions. We can use translational invariance to put all four operators at the same position $\boldsymbol{r}$. Three of the integrals over space then give momentum-conserving delta functions. The resulting expression for the factor in Eq. (13) that involves matrix elements of C is

$$\begin{aligned}\sum_f \left| \sum_m \frac{\langle f|C|m\rangle\langle m|C|i\rangle}{\omega_{mi} \pm \omega} \right|^2 \;=\; & \sum_f (2\pi)^3 \delta^3(\boldsymbol{K}_f - \boldsymbol{K}_i) \int d^3r \\ & \times \sum_m (2\pi)^3 \delta^3(\boldsymbol{K}_m - \boldsymbol{K}_i) \; \frac{\langle f|\mathcal{C}(\boldsymbol{r})|m\rangle\langle m|\mathcal{C}(\boldsymbol{r})|i\rangle}{\omega_{mi} \pm \omega} \\ & \times \sum_{m'} (2\pi)^3 \delta^3(\boldsymbol{K}_{m'} - \boldsymbol{K}_i) \frac{\langle i|\mathcal{C}(\boldsymbol{r})|m'\rangle\langle m'|\mathcal{C}(\boldsymbol{r})|f\rangle}{\omega_{m'i} \pm \omega}, \end{aligned} \tag{17}$$

where $\boldsymbol{K}_m$ and $\boldsymbol{K}_{m'}$ are the total momenta of the intermediate states $|m\rangle$ and $|m'\rangle$, respectively. Homogeneity implies that the integrand is independent of the position $\boldsymbol{r}$. Thus the integral $\int d^3r$ just gives a factor of the volume V.

E. Local Density Approximation

For a many-body system whose number density varies slowly with the position $\boldsymbol{r}$, the transition rate can be simplified by using the *local density approximation*. The transition rate is an extensive quantity. For a homogeneous system, the expressions obtained by inserting Eq. (16) or Eq. (17) into the transition rate have an explicit factor of the volume $\int d^3r = V$. If the transition rate is also proportional to the total number N_i of some type of particle, the additional factor must be the intensive combination N_i/V. For a homogeneous system consisting of fermionic atoms with spin states 1 and 2, the association rate is proportional to $N_1 N_2$. The local density approximation for the association rate in a system with local number densities $n_1(\boldsymbol{r})$ and $n_2(\boldsymbol{r})$ can be obtained by making the substitution

$$N_1 N_2/V \longrightarrow \int d^3r \, n_1(\boldsymbol{r}) n_2(\boldsymbol{r}). \tag{18}$$

For a homogeneous system consisting of dimers, the disssociation rate is proportional to their total number $N_{\rm D}$. The local density approximation for the disssociation rate in a system with local number density $n_{\rm D}(\boldsymbol{r})$ can be obtained by making the substitution

$$N_{\rm D} \longrightarrow \int d^3r \, n_{\rm D}(\boldsymbol{r}). \tag{19}$$

III. HARMONIC ASSOCIATION RATE

A pair of atoms with a large positive scattering length can be associated into a universal dimer by an oscillating magnetic field. In this section, we calculate the harmonic association rate in a thermal gas of atoms. We also give the subharmonic association rate from first-order perturbation theory. We consider a gas of atoms that is in thermal equilibrium at

temperature T. For simplicity, we take the number densities n_1 and n_2 of the atoms to be sufficiently low that their distributions are given by Boltzmann statistics instead of Fermi-Dirac statistics.

A. Initial and Final States

We first consider a homogeneous gas consisting of N_1 atoms of spin state 1 and N_2 atoms of spin state 2 in a volume V. The two spin states interact with a large positive scattering length $\bar{a}$. The universal dimer has a small binding energy $\hbar^2/m\bar{a}^2$. For a gas in thermal equilibrium, the harmonic transition rate is given by Eq. (8) with the substitution in Eq. (14), where $\rho = \rho_{\rm gas}$ is the density matrix for the thermal gas of atoms. To simplify the presentation, we will temporarily ignore the frequency delta function, which depends on the energy E_i of the states in the density matrix. The terms in Eq. (8) that depend on the contact operator can then be expressed compactly as $\sum_f \langle f|C\rho_{\rm gas}C|f\rangle$. We will insert the frequency delta function at the end of the calculation.

In the low-density limit where 3-body and higher-body correlations can be neglected, the density matrix $\rho_{\rm gas}$ can be expressed in terms of the density matrix $\rho_{\rm pair}$ for a pair of atoms in thermal equilibrium:

$$\sum_f \langle f|C\rho_{\rm gas}C|f\rangle = N_1N_2 \sum_f \langle f|C\rho_{\rm pair}C|f\rangle. \tag{20}$$

The factor N_1N_2 is the number of pairs of fermions in the two spin states. (For a gas of N identical bosons, the number of pairs is $N^2/2$.) The pair density matrix is normalized: $\mathrm{Tr}(\rho_{\rm pair}) = 1$. On the left side of Eq. (20), the sum over f is over many-body final states that include a single dimer. On the right side, the sum over f is over two-atom final states that consist of a single dimer. The density matrix for a pair of atoms in thermal equilibrium is

$$\rho_{\rm pair} = \frac{\lambda_{\rm T}^6}{V^2} \int_{\boldsymbol{K}} \int_{\boldsymbol{k}} \exp(-\beta\hbar^2K^2/4m - \beta\hbar^2k^2/m)|\boldsymbol{K},\boldsymbol{k}\rangle\langle\boldsymbol{k},\boldsymbol{K}|, \tag{21}$$

where $\beta = 1/k_BT$ and $\lambda_{\rm T}$ is the thermal deBroglie wavelength for an atom with mass m:

$$\lambda_{\rm T} = \sqrt{2\pi\hbar^2/mk_{\rm B}T}. \tag{22}$$

The two-atom states $|\boldsymbol{K},\boldsymbol{k}\rangle$ in Eq. (21) are labeled by the center-of-mass wave vector $\boldsymbol{K} = \boldsymbol{k}_1 + \boldsymbol{k}_2$ and the relative wave vector $\boldsymbol{k} = (\boldsymbol{k}_1 - \boldsymbol{k}_2)/2$. The integrals over the wave vectors are defined by

$$\int_{\boldsymbol{k}} \equiv \int \frac{d^3k}{(2\pi)^3}. \tag{23}$$

The wave vector states have delta-function normalizations: $\langle\boldsymbol{k}'|\boldsymbol{k}\rangle = (2\pi)^3\delta^3(\boldsymbol{k}' - \boldsymbol{k})$. In the case $\boldsymbol{k}' = \boldsymbol{k}$, the infinite norm can be expressed as a factor of the volume: $\langle\boldsymbol{k}|\boldsymbol{k}\rangle = V$. The energy of a pair of atoms in the state $|\boldsymbol{K},\boldsymbol{k}\rangle$ is

$$E_{\rm AA} = \hbar^2K^2/4m + \hbar^2k^2/m. \tag{24}$$

The sum over final states on the right hand side of Eq. (20) can be expressed as an integral over the wave vector $\boldsymbol{k}_{\rm D}$ of a dimer:

$$\sum_f \langle f|C\rho_{\rm pair}C|f\rangle = \int_{\boldsymbol{k}_{\rm D}} \langle\boldsymbol{k}_{\rm D}|C\rho_{\rm pair}C|\boldsymbol{k}_{\rm D}\rangle. \tag{25}$$

The energy of the dimer is

$$E_{\rm D} = -\hbar^2/m\bar{a}^2 + \hbar^2 k_{\rm D}^2/4m. \tag{26}$$

B. Matrix Elements

Because the system is homogeneous, the analog of Eq. (16) can be used to express the contact operators C on the right side of Eq. (25) in terms of contact density operators at the same position $\boldsymbol{r}$. The wave vector delta function in Eq. (16) reduces to $\delta^3(\boldsymbol{k}_{\rm D} - \boldsymbol{K})$, and it can be used to integrate over $\boldsymbol{k}_{\rm D}$. The frequency delta function in Eq. (8) reduces to

$$\sum_{\pm} 2\pi\delta\big((E_{\rm D} - E_{\rm AA})/\hbar \pm \omega\big) = 2\pi\delta\big(\omega - \hbar/m\bar{a}^2 - \hbar k^2/m\big). \tag{27}$$

In the sum over $\pm\omega$, only the $+\omega$ term contributes.

The expression for the transition rate has been reduced to matrix elements of the contact density operator of the form $\langle \boldsymbol{k}_{\rm D}|\mathcal{C}(\boldsymbol{r})|\boldsymbol{K},\boldsymbol{k}\rangle$. The matrix element is calculated in Appendix B, and is given by Eq. (B12):

$$\langle \boldsymbol{k}_{\rm D}|\mathcal{C}(\boldsymbol{r})|\boldsymbol{K},\boldsymbol{k}\rangle = \frac{\sqrt{128\pi^3\bar{a}}}{1 - i\bar{a}k}. \tag{28}$$

The Gaussian integral over $\boldsymbol{K}$ can be evaluated analytically. The sum over final states of the matrix element in Eq. (25) reduces to

$$\sum_f \langle f|C\rho_{\rm gas}C^\dagger|f\rangle = 128\sqrt{2}\pi\bar{a}\lambda_{\rm T}^3 \frac{N_1N_2}{V}\int_0^\infty dk \frac{k^2}{1 + k^2\bar{a}^2}\exp(-\beta\hbar^2k^2/m). \tag{29}$$

Before integrating over k, this must be multiplied by the frequency delta function in Eq. (27).

C. Harmonic Association Rate

Our final result for the harmonic association rate $\Gamma_1^{(1)}(\omega)$ in the homogeneous gas can be obtained from Eq. (8) by replacing $\sum_f |\langle f|C|i\rangle|^2$ by the right side of Eq. (29), replacing the sum of frequency delta functions by the right side of Eq. (27), and then using the delta function to integrate over k. The local density approximation can be implemented by making the substitution for N_1N_2/V in Eq. (18). The threshold angular frequency for association is $\hbar/m\bar{a}^2$: the emission of a smaller energy from a pair of atoms is not enough to allow a transition to dimer. For $\omega > \hbar/m\bar{a}^2$, the harmonic association rate is

$$\Gamma_1^{(1)}(\omega) = \frac{2\sqrt{2}\hbar^2}{m^2a_{\rm bg}^2\bar{a}}\left(\frac{b\Delta}{(\Delta + B_0 - \bar{B})^2}\right)^2\left(\int d^3r\, n_1(\boldsymbol{r})n_2(\boldsymbol{r})\right)\frac{\lambda_{\rm T}^3\kappa(\omega)}{\omega}\exp(-\beta\hbar^2\kappa^2(\omega)/m), \tag{30}$$

where

$$\kappa(\omega) = \sqrt{m\omega/\hbar - 1/\bar{a}^2}. \tag{31}$$

(The harmonic association rate in a thermal gas of identical bosons with large scattering length was calculated in Ref. [15]. It can be obtained from Eq. (30) by replacing $n_1(\boldsymbol{r})n_2(\boldsymbol{r})$ by $n^2(\boldsymbol{r})/2$, where $n(\boldsymbol{r})$ is the local number density of identical bosons.) If $k_BT \ll \hbar^2/m\bar{a}^2$, the harmonic association rate in Eq. (30) has a narrow peak with a maximum when ω is above the threshold $\hbar/m\bar{a}^2$ by approximately $\frac{1}{2}(k_BT/\hbar)$. For large frequency, the rate decreases as $\exp(-\hbar\omega/k_BT)$.

D. First-Order Subharmonic Association Rate

According to Eq. (11), the contribution $\Gamma_2^{(2)}(\omega)$ to the subharmonic association rate from the first-order perturbation in H_2 can be expressed in terms of the harmonic association rate in Eq. (30) at twice the frequency. The threshold angular frequency for subharmonic association is $\frac{1}{2}(\hbar/m\bar{a}^2)$. For $\omega > \frac{1}{2}(\hbar/m\bar{a}^2)$, the subharmonic association rate is

$$\Gamma_2^{(2)}(\omega) = \frac{\sqrt{2}\hbar^2}{4m^2 a_{\rm bg}^2 \bar{a}} \left(\frac{b^2\Delta}{(\Delta + B_0 - \bar{B})^3}\right)^2 \left(\int d^3r\, n_1(\boldsymbol{r}) n_2(\boldsymbol{r})\right) \frac{\lambda_{\rm T}^3 \kappa(2\omega)}{\omega} \exp(-\beta\hbar^2\kappa^2(2\omega)/m), \tag{32}$$

where $\kappa(2\omega)$ is the function defined in Eq. (31) with ω replaced by 2ω:

$$\kappa(2\omega) = \sqrt{2m\omega/\hbar - 1/\bar{a}^2}. \tag{33}$$

If $k_B T \ll \hbar^2/m\bar{a}^2$, this contribution to the subharmonic association rate has a narrow peak with a maximum when ω is above the threshold $\frac{1}{2}(\hbar/m\bar{a}^2)$ by approximately $\frac{1}{4}(k_B T/\hbar)$. The height of the peak is smaller than that of the harmonic association rate by the factor $[b/(\Delta + B_0 - \bar{B})]^2/4$.

IV. HARMONIC DISSOCIATION RATE

A universal dimer can be dissociated by an oscillating magnetic field into its constituent atoms. In this section, we calculate the harmonic dissociation rate in a thermal gas of dimers. We also give the subharmonic dissociation rate from first-order perturbation theory. We consider a gas of dimers in thermal equilibrium at temperature T. For simplicity, we take the number density $n_{\rm D}$ of dimers to be sufficiently low that their distribution is given by Boltzmann statistics instead of Bose-Einstein statistics.

A. Initial and Final States

We first consider a homogeneous gas consisting of $N_{\rm D}$ dimers in a volume V. If the gas is in thermal equilibrium, the harmonic transition rate is given by Eq. (8) with the substitution in Eq. (14), where $\rho_{\rm gas}$ is the density matrix for the thermal gas of dimers. To simplify the presentation, we will temporarily ignore the frequency delta function, which depends on the energy E_i of the states in the density matrix. The terms in Eq. (8) that depend on the contact operator can be expressed compactly as $\sum_f \langle f|C\rho_{\rm gas}C|f\rangle$. We will insert the frequency delta function at the end of the calculation.

In the low-density limit where correlations between dimers can be neglected, the density matrix $\rho_{\rm gas}$ can be expressed in terms of the density matrix $\rho_{\rm dimer}$ for a single dimer in thermal equilibrium:

$$\sum_f \langle f|C\rho_{\rm gas}C|f\rangle = N_{\rm D} \sum_f \langle f|C\rho_{\rm dimer}C|f\rangle. \tag{34}$$

The dimer density matrix is normalized: $\mathrm{Tr}(\rho_{\rm dimer}) = 1$. On the left side of Eq. (34), the sum over f is over many-body final states that include an unbound pair of atoms. On the

right side, the sum over f is over two-atom final states that consist of an unbound pair of atoms. The density matrix for a dimer in thermal equilibrium is

$$\rho_{\rm dimer} = \frac{\lambda_T^3}{2\sqrt{2}V} \int_{\boldsymbol{k}_{\rm D}} \exp\left(-\beta\hbar^2 k_{\rm D}^2/4m\right)\ |\boldsymbol{k}_{\rm D}\rangle\langle\boldsymbol{k}_{\rm D}|, \tag{35}$$

where $\lambda_{\rm T}$ is the thermal deBroglie wavelength for an atom in Eq. (22). The energy $E_{\rm D}$ of the dimer is given in Eq. (26).

The sum over final states on the right side of Eq. (34) can be expressed as integrals over the total wave vector and the relative wave vector of a pair of atoms:

$$\sum_f \langle f|C\rho_{\rm dimer}C|f\rangle = \int_{\boldsymbol{K}} \int_{\boldsymbol{k}} \langle \boldsymbol{K},\boldsymbol{k}|C\rho_{\rm dimer}C|\boldsymbol{K},\boldsymbol{k}\rangle. \tag{36}$$

The energy $E_{\rm AA}$ of the pair of atoms is given in Eq. (24).

B. Matrix Elements

Because the system is homogeneous, the analog of Eq. (16) can be used to express the contact operators C on the right side of Eq. (36) in terms of contact density operators at the same position $\boldsymbol{r}$. The wave-vector delta function in Eq. (16) reduces to $\delta^3(\boldsymbol{K}-\boldsymbol{k}_{\rm D})$, and it can be used to integrate over $\boldsymbol{K}$. The frequency delta function in Eq. (8) reduces to

$$\sum_{\pm} 2\pi\delta\big((E_{\rm AA}-E_{\rm D})/\hbar \pm \omega\big) = 2\pi\delta\big(\omega - \hbar/m\bar{a}^2 - \hbar k^2/m\big). \tag{37}$$

In the sum over $\pm\omega$, only the $-\omega$ term contributes.

The expression for the transition rate has been reduced to matrix elements of the contact density operator of the form $\langle \boldsymbol{K},\boldsymbol{k}|\mathcal{C}(\boldsymbol{r})|\boldsymbol{k}_{\rm D}\rangle$. The matrix element is the complex conjugate of Eq. (28). The Gaussian integral over $\boldsymbol{K}$ can be evaluated analytically. The sum over final states of the matrix element in Eq. (36) reduces to

$$\sum_f \big|\langle f|C\rho_{\rm gas}C|f\rangle\big| = 64\pi N_{\rm D} \int_0^\infty dk\ \frac{k^2\bar{a}}{1+k^2\bar{a}^2}\ . \tag{38}$$

Before integrating over k, this must be multiplied by the frequency delta function in Eq. (37).

C. Harmonic Dissociation Rate

Our final result for the harmonic disssociation rate $\Gamma_1^{(1)}(\omega)$ in the homogeneous gas can be obtained from Eq. (8) by replacing $\sum_f |\langle f|C|i\rangle|^2$ by the right side of Eq. (38), replacing the sum of frequency delta functions by the right side of Eq. (37), and then using the delta function to integrate over k. The local density approximation can be implemented by making the substitution for $N_{\rm D}$ in Eq. (19). The threshold angular frequency for dissociation is $\hbar/m\bar{a}^2$: the absorption of smaller energy is not enough to break up the dimer. For $\omega > \hbar/m\bar{a}^2$, the harmonic dissociation rate is

$$\Gamma_1^{(1)}(\omega) = \frac{\hbar^2}{m^2 a_{\rm bg}^2 \bar{a}} \left(\frac{b\Delta}{(\Delta+B_0-\bar{B})^2}\right)^2 \left(\int d^3r\, n_{\rm D}(\boldsymbol{r})\right) \frac{(m\omega/\hbar - 1/\bar{a}^2)^{1/2}}{\omega}. \tag{39}$$

(If the universal dimers are composed of identical bosons, the harmonic dissociation rate is given by this same expression.) The harmonic dissociation rate in Eq. (39) has a maximum at $\omega = 2(\hbar/m\bar{a}^2)$, which is twice the threshold angular frequency. For large frequency, the rate decreases very slowly as $\omega^{-1/2}$. The dissociation rate is independent of the temperature T. This may be surprising at first, but it is related to the fact that the contact of a thermal gas of dimers is independent of T.

D. First-Order Subharmonic Dissociation Rate

According to Eq. (11), the contribution $\Gamma_2^{(2)}(\omega)$ to the subharmonic dissociation rate from the first-order perturbation in H_2 can be expressed in terms of the harmonic dissociation rate in Eq. (39) at twice the frequency. The threshold angular frequency for subharmonic dissociation is $\frac{1}{2}(\hbar/m\bar{a}^2)$. For $\omega > \frac{1}{2}(\hbar/m\bar{a}^2)$, the transition rate is

$$\Gamma_2^{(2)}(\omega) = \frac{\hbar^2}{8m^2 a_{\rm bg}^2 \bar{a}} \left(\frac{b^2\Delta}{(\Delta + B_0 - \bar{B})^3} \right)^2 \left(\int d^3r \, n_{\rm D}(\boldsymbol{r}) \right) \frac{(2m\omega/\hbar - 1/\bar{a}^2)^{1/2}}{\omega}. \tag{40}$$

This contribution to the subharmonic dissociation rate has a maximum at $\omega = \hbar/m\bar{a}^2$, which is twice the threshold angular frequency. The height of the peak is smaller than that of the harmonic dissociation rate by a factor of $[b/(\Delta + B_0 - \bar{B})]^2/4$.

V. SUBHARMONIC ASSOCIATION RATE

In this section, we calculate the subharmonic association rate in a thermal gas of atoms from the second-order perturbation in H_1. We will find that this contribution is much larger than that from the first-order perturbation in H_2 if $\bar{B}$ is near a Feshbach resonance.

A. Initial, Final, and Intermediate States

We first consider a homogeneous gas consisting of N_1 atoms of spin state 1 and N_2 atoms of spin state 2 in a volume V. If the gas is in thermal equilibrium, the harmonic transition rate is given by Eq. (13) with the substitution in Eq. (14), where $\rho = \rho_{\rm gas}$ is the density matrix for the thermal gas of atoms. In the low-density limit where 3-body and higher-body correlations can be neglected, the density matrix $\rho_{\rm gas}$ can be expressed in terms of the density matrix $\rho_{\rm pair}$ for a pair of atoms in thermal equilibrium, as in Eq. (20). That density matrix $\rho_{\rm pair}$ is given in Eq. (21). The sum over final states reduces to an integral over the wave vector $\boldsymbol{k}_{\rm D}$ of the dimer, as in Eq. (25).

Once the matrix elements have been reduced to matrix elements in the two-atom sector, the sum over intermediate states in Eq. (13) reduces to a sum over atom-pair states and dimer states. If the initial state is an atom pair with total energy $E_{\rm AA}$, the sum over states is

$$\sum_m \frac{|m\rangle\langle m|}{\omega_{mi} \pm \omega} = \int_{\boldsymbol{K}'} \int_{\boldsymbol{k}'} \frac{|\boldsymbol{K}', \boldsymbol{k}'\rangle\langle \boldsymbol{k}', \boldsymbol{K}'|}{(E'_{\rm AA} - E_{\rm AA})/\hbar \pm \omega} + \int_{\boldsymbol{k}'_{\rm D}} \frac{|\boldsymbol{k}'_{\rm D}\rangle\langle \boldsymbol{k}'_{\rm D}|}{(E'_{\rm D} - E_{\rm AA})/\hbar \pm \omega}, \tag{41}$$

where $E'_{\rm AA}$ and $E'_{\rm D}$ are given by Eqs. (24) and (26) with primes on the wavenumber variables. In the transition rate given by inserting Eq. (17) into Eq. (13), there are four possibilities

for the intermediate states $|m\rangle$ and $|m'\rangle$ in the amplitude and its complex conjugate: each one can be either an atom pair or a dimer. The transition rate can be expressed accordingly as the sum of four terms:

$$\Gamma_2^{(1,1)} = \Gamma_{\mathrm{AA,AA}} + \Gamma_{\mathrm{D,D}} + \Gamma_{\mathrm{AA,D}} + \Gamma_{\mathrm{D,AA}}. \tag{42}$$

We will calculate each of these terms individually.

B. Matrix Elements

Because the system is homogeneous, the matrix elements of the contact C in Eq. (13) can be expressed in terms of matrix elements of the contact density operator using Eq. (17). In addition to the matrix element in Eq. (28) and its complex conjugate, we also need the matrix elements of $\mathcal{C}(\boldsymbol{r})$ between atom-pair states and between dimer states. They are calculated in Appendix B and given in Eqs. (B11) and Eqs. (B13):

$$\langle \boldsymbol{K}', \boldsymbol{k}'|\mathcal{C}(\boldsymbol{r})|\boldsymbol{K}, \boldsymbol{k}\rangle = \frac{16\pi^2\bar{a}^2}{(1+i\bar{a}k')(1-i\bar{a}k)}, \tag{43a}$$

$$\langle \boldsymbol{k}'_{\mathrm{D}}|\mathcal{C}(\boldsymbol{r})|\boldsymbol{k}_{\mathrm{D}}\rangle = 8\pi/\bar{a}. \tag{43b}$$

The integrals over the total wave vectors of the intermediate states and over the wave vector of the final-state dimer can be evaluated using the delta functions in Eq. (17). The Gaussian integral over the total wave vector of the initial atom-pair state can then be evaluated analytically. The frequency delta function reduces to

$$\sum_{\pm} 2\pi\delta\big((E_{\mathrm{D}} - E_{\mathrm{AA}})/\hbar \pm 2\omega\big) = 2\pi\delta\big(2\omega - \hbar/m\bar{a}^2 - \hbar k^2/m\big). \tag{44}$$

In the sum over $\pm 2\omega$, only the $+2\omega$ term contributes.

1. *Intermediate atom-pair states*

The contribution from intermediate atom-pair states to the factor in the transition rate involving matrix elements reduces to

$$\sum_i \sum_f \left| \sum_m \frac{\langle f|C|m\rangle\langle m|C|i\rangle}{\omega_{mi}+\omega} \right|^2 N_1 N_2 \langle i|\rho_{\mathrm{pair}}|i\rangle = 8192\sqrt{2}\pi \frac{m^2\lambda_{\mathrm{T}}^3}{\hbar^2\bar{a}} \frac{N_1 N_2}{V} \times \int_0^\infty dk \frac{k^2 \exp(-\beta\hbar^2k^2/m)}{k^2+1/\bar{a}^2} \left[\int_0^\infty dk' \frac{k'^2}{(k'^2+1/\bar{a}^2)(k'^2-k^2+m\omega/\hbar)} \right]^2. \tag{45}$$

Before integrating over k, this must be multiplied by the frequency delta function in Eq. (44).

The threshold angular frequency for subharmonic association is $\frac{1}{2}(\hbar/m\bar{a}^2)$. For $\omega > \hbar/m\bar{a}^2$, the integral over k' in Eq. (45) has a pole on the integration contour. In this region of ω, this contribution to the transition rate is a subleading correction of order b^4 to the harmonic transition rate of order b^2 in Eq. (30). We therefore consider only the frequency

interval $\frac{1}{2}(\hbar/m\bar{a}^2) < \omega < \hbar/m\bar{a}^2$, where this contribution to the transition rate is leading order in b. In this region of ω, the integral over $k^{'}$ in Eq. (45) is

$$\int_0^\infty dk^{'} \frac{k^{'2}}{(k^{'2}+1/\bar{a}^2)(k^{'2}-k^2+m\omega/\hbar)} = \frac{\pi\bar{a}}{2\big(1+\bar{a}\sqrt{m\omega/\hbar-k^2}\,\big)}. \tag{46}$$

The frequency delta function in Eq. (44) can be used to evaluate the integral over k in Eq. (45). The resulting contribution to the transition rate is

$$\Gamma_{\rm AA,AA} = \frac{\sqrt{2}\hbar^2\lambda_T^3\bar{a}}{4m^2a_{\rm bg}^4}\left(\frac{b\Delta}{(\Delta+B_0-\bar{B})^2}\right)^4 \frac{N_1N_2}{V}\frac{\kappa(2\omega)\exp\big(-\beta\hbar^2\kappa^2(2\omega)/m\big)}{\omega\big(1+\sqrt{1-m\omega\bar{a}^2/\hbar}\,\big)^2}, \tag{47}$$

where $\kappa(2\omega)$ is given in Eq. (33).

2. Intermediate dimer states

The contribution from intermediate dimer states to the factor in the transition rate involving matrix elements reduces to

$$\begin{aligned}\sum_i\sum_f\left|\sum_m \frac{\langle f|C|m\rangle\langle m|C|i\rangle}{\omega_{mi}+\omega}\right|^2 N_1N_2\langle i|\rho_{\rm pair}|i\rangle \\ = 8192\sqrt{2}\pi^3\frac{m^2\lambda_{\rm T}^3}{\hbar^2\bar{a}^3}\frac{N_1N_2}{V}\int_0^\infty dk\frac{k^2\exp(-\beta\hbar^2k^2/m)}{(k^2+1/\bar{a}^2)(k^2+1/\bar{a}^2-m\omega/\hbar)^2}.\end{aligned} \tag{48}$$

Before integrating over k, this must be multiplied by the frequency delta function in Eq. (44). The frequency delta function can be used to evaluate the integral over k in Eq. (48). The resulting contribution to the transition rate is

$$\Gamma_{\rm D,D} = \frac{\sqrt{2}\hbar^4\lambda_T^3}{m^4a_{\rm bg}^4\bar{a}^3}\left(\frac{b\Delta}{(\Delta+B_0-\bar{B})^2}\right)^4 \frac{N_1N_2}{V}\frac{\kappa(2\omega)}{\omega^3}\exp\big(-\beta\hbar^2\kappa^2(2\omega)/m\big). \tag{49}$$

3. Interference between Atom-Pair and Dimer States

The contribution to the factor in the transition rate involving matrix elements from intermediate atom-pair states in the amplitude and from intermediate dimer states in its complex conjugate reduces to

$$\begin{aligned}\sum_i\sum_f\sum_m \frac{\langle f|C|m\rangle\langle m|C|i\rangle}{\omega_{mi}+\omega}\sum_{m'}\frac{\langle i|C|m'\rangle\langle m'|C|f\rangle}{\omega_{m'i}+\omega}N_1N_2\langle i|\rho_{\rm pair}|i\rangle \\ = -8192\sqrt{2}\pi^2\frac{m^2\lambda_{\rm T}^2}{\hbar^2\bar{a}^2}\frac{N_1N_2}{V}\int_0^\infty dk\frac{k^2\exp(-\beta\hbar^2k^2/m)}{(k^2+1/\bar{a}^2)(k^2+1/\bar{a}^2-\omega/\hbar)} \\ \times\int_0^\infty dk^{'}\frac{k^{'2}}{(k^{'2}+1/\bar{a}^2)(k^{'2}-k^2+m\omega/\hbar)}.\end{aligned} \tag{50}$$

Before integrating over k, this must be multiplied by the frequency delta function in Eq. (44). The integral over k' is given in Eq. (46). The frequency delta function can be used to evaluate the integral over k in Eq. (48). The resulting contribution to the transition rate is

$$\Gamma_{\rm AA,D} = -\frac{\hbar^3\lambda_T^3}{\sqrt{2}m^3a_{\rm bg}^4\bar{a}}\left(\frac{b\Delta}{(\Delta+B_0-\bar{B})^2}\right)^4 \frac{N_1N_2}{V}\frac{\kappa(2\omega)\exp\big(-\beta\hbar^2\kappa^2(2\omega)/m\big)}{\omega^2\big(1+\sqrt{1-m\omega\bar{a}^2/\hbar}\,\big)}. \tag{51}$$

The contribution $\Gamma_{\rm D,AA}$ from intermediate dimer states in the amplitude and intermediate atom-pair states in its complex conjugate is the same as Eq. (51) for frequencies in the range $\frac{1}{2}(\hbar/m\bar{a}^2) < \omega < \hbar/m\bar{a}^2$. The contributions $\Gamma_{\rm AA,D} = \Gamma_{\rm D,AA}$ are negative, because there is destructive interference between atom-pair and dimer intermediate states.

C. Total subharmonic transition rate

The total subharmonic transition rate in Eq. (42) from the second-order perturbation in H_1 is given by adding Eqs. (47) and (49) and twice Eq. (51). The local density approximation can be implemented by making the substitution for N_1N_2/V in Eq. (18). For frequencies in the range $\frac{1}{2}(\hbar/m\bar{a}^2) < \omega < \hbar/m\bar{a}^2$, the subharmonic transition rate is

$$\begin{aligned}\Gamma_2^{(1,1)}(\omega) \;=\; & \frac{\sqrt{2}\hbar^2\bar{a}}{4m^2a_{\rm bg}^4}\left(\frac{b\Delta}{(\Delta+B_0-\bar{B})^2}\right)^4\left(\int d^3r\;\; n_1(\boldsymbol{r})n_2(\boldsymbol{r})\right) \\ & \times\frac{\lambda_T^3\kappa(2\omega)}{\omega}\exp\big(-\beta\hbar^2\kappa^2(2\omega)/m\big)\left(\frac{1}{1+\sqrt{1-m\omega\bar{a}^2/\hbar}}-\frac{2}{m\omega\bar{a}^2/\hbar}\right)^2,\end{aligned} \tag{52}$$

where $\kappa(2\omega)$ is given by Eq. (33). (The corresponding result for identical bosons can be obtained by replacing $n_1(\boldsymbol{r})n_2(\boldsymbol{r})$ by $n^2(\boldsymbol{r})/2$, where $n(\boldsymbol{r})$ is the local number density.)

If $k_BT \ll \hbar^2/m\bar{a}^2$, the subharmonic association rate in Eq. (52) has a narrow peak with a maximum when ω is above the threshold $\frac{1}{2}(\hbar/m\bar{a}^2)$ by approximately $\frac{1}{4}(k_BT/\hbar)$. In the region near the threshold and the peak, the largest contribution comes from intermediate dimer states. The intermediate atom-pair states give a contribution that is smaller at threshold by a factor of $(3-2\sqrt{2})/8 \approx 0.021$. The cross terms give a negative contribution that is smaller at threshold by a factor of $(2-\sqrt{2})/2 \approx 0.29$. The subharmonic association rate in Eq. (52) is much smaller than the harmonic association rate in Eq. (30). The ratio of their maximum values is

$$\frac{\Gamma_{2,\rm max}^{(1,1)}}{\Gamma_{1,\rm max}^{(1)}} = 2.914\left(\frac{b\Delta}{(\Delta+B_0-\bar{B})^2}\right)^2\left(\frac{\bar{a}}{a_{\rm bg}}\right)^2\left(1-1.21\frac{k_BTm\bar{a}^2}{\hbar^2}+\ldots\right). \tag{53}$$

The contribution $\Gamma_2^{(2)}$ to the subharmonic transition rate from the first-order perturbation in H_2 is given in Eq. (32). Near the subharmonic threshold frequency, $\Gamma_2^{(1,1)}$ differs from $\Gamma_2^{(2)}$ by a factor of $11.6\,(\bar{a}/a_{\rm bg})^2[\Delta/(\Delta+B_0-\bar{B})]^2$. If $\bar{B}$ is near the Feshbach resonance, $\Gamma_2^{(2)}$ is much smaller. It is therefore unnecessary to consider interference between the first-order perturbation in H_1 and the second-order perturbation in H_2.

VI. SUBHARMONIC DISSOCIATION RATE

In this section, we calculate the subharmonic dissociation rate in a thermal gas of dimers from the second-order perturbation in H_1. We first consider a homogeneous gas of $N_{\rm D}$ dimers in a volume V in thermal equilibrium at temperature T. The subharmonic transition rate is given by Eq. (13) with Eq. (17) inserted and with $|i\rangle\langle i|$ replaced by the density matrix $\rho_{\rm gas}$ for the thermal gas of dimers. In the low-density limit where correlations between dimers can be neglected, $\rho_{\rm gas}$ can be expressed in terms of the density matrix $\rho_{\rm dimer}$ for a dimer in thermal equilibrium, as in Eq. (34). The density matrix $\rho_{\rm dimer}$ is given in Eq. (35). The sum over final states reduces to an integral over center-of-mass wave vector K and relative wave vector k of a pair of atoms, as in Eq. (36). The frequency delta function reduces to

$$\sum_{\pm} 2\pi\delta\big((E_{\rm AA}-E_{\rm D})/\hbar \pm 2\omega\big) = 2\pi\delta\big(2\omega - \hbar/m\bar{a}^2 - \hbar k^2/m\big). \tag{54}$$

In the sum over $\pm 2\omega$, only the -2ω term contributes. In the sums over intermediate states in the amplitude and its complex conjugate, both intermediate states can be either an atom pair or a dimer. The calculation of the individual contributions proceeds in the same way as for the association rate. They can be obtained from those in Eqs. (47), (49), and (51) by replacing N_1N_2/V by $N_{\rm D}$ and replacing $\lambda_{\rm T}^3 \exp\big(-\beta\hbar^2\kappa^2(2\omega)/m\big)$ by $\sqrt{2}/4$.

In the local density approximation, the factor $N_{\rm D}$ is replaced by $\int d^3r\, n_{\rm D}(\boldsymbol{r})$. For frequencies in the range $\frac{1}{2}(\hbar/m\bar{a}^2) < \omega < \hbar/m\bar{a}^2$, the subharmonic dissociation rate is

$$\Gamma_2^{(1,1)}(\omega) \;=\; \frac{\hbar^2\bar{a}}{8m^2a_{\rm bg}^4}\left(\frac{b\Delta}{(\Delta+B_0-\bar{B})^2}\right)^4 \left(\int d^3r\;\; n_{\rm D}(\boldsymbol{r})\right) \times\frac{\kappa(2\omega)}{\omega}\left(\frac{1}{1+\sqrt{1-m\omega\bar{a}^2/\hbar}} - \frac{2}{m\omega\bar{a}^2/\hbar}\right)^2, \tag{55}$$

where $\kappa(2\omega)$ is given by Eq. (33). (If the universal dimers are composed of identical bosons, the subharmonic dissociation rate is given by this same expression.) Like the harmonic dissociation rate in Eq. (39), the subharmonic dissociation rate in Eq. (55) is independent of the temperature T. The subharmonic dissociation rate has a maximum at an angular frequency ω that is above the threshold $\frac{1}{2}(\hbar/m\bar{a}^2)$ by approximately $0.082(\hbar/m\bar{a}^2)$. The subharmonic dissociation rate in Eq. (52) is much smaller than the harmonic dissociation rate in Eq. (39). The ratio of their maximum values is

$$\frac{\Gamma_{2,\rm max}^{(1,1)}}{\Gamma_{1,\rm max}^{(1)}} = 1.39\left(\frac{b\Delta}{(\Delta+B_0-\bar{B})^2}\right)^2\left(\frac{\bar{a}}{a_{\rm bg}}\right)^2. \tag{56}$$

The contribution $\Gamma_2^{(2)}$ to the subharmonic transition rate from the first-order perturbation in H_2 is given in Eq. (40). Near the subharmonic threshold frequency, $\Gamma_2^{(1,1)}$ differs from $\Gamma_2^{(2)}$ by a factor of $11.6\,(\bar{a}/a_{\rm bg})^2[\Delta/(\Delta+B_0-\bar{B})]^2$. If $\bar{B}$ is near the Feshbach resonance, $\Gamma_2^{(2)}$ is much smaller. It is therefore unnecessary to consider interference between the first-order perturbation in H_1 and the second-order perturbation in H_2.

VII. PREVIOUS EXPERIMENTS WITH ULTRACOLD ATOMS

In this section, we briefly describe previous experiments on the association of atoms into molecules using longitudinal modulation of the magnetic field. The association of atoms into molecules was observed through the loss of trapped atoms, presumably from inelastic collisions of the molecules with atoms. The number of atoms remaining in the trap after some modulation time was measured as a function of the oscillation frequency. A loss resonance provided the signature for the molecule. The first such experiments were carried out at JILA in Boulder using ^{85}Rb atoms [1] and using a mixture of ^{85}Rb and ^{87}Rb atoms [3]. An experiment using a mixture of ^{41}K and ^{87}Rb atoms was carried out at LENS in Florence [4]. An experiment using ^{133}Cs atoms was carried out at University of Innsbruck [5]. Experiments using ^{7}Li atoms have been carried out at Bar-Ilan University [7–9] and at Rice University [10]. After describing those experiments, we illustrate our theoretical results for association and dissociation rates using the conditions of the Rice University experiment.

A. JILA Experiments

The measurements of the binding energies of dimers using longitudinal modulation of the magnetic field was pioneered by Thompson, Hodby, and Wieman using ^{85}Rb atoms [1]. The scattering length was controlled using the Feshbach resonance at 155.0 G for ^{85}Rb atoms in the $|F = 2, m_F = -2\rangle$ hyperfine state. The measurements were made on thermal gases of trapped atoms with temperatures ranging from 20 to 80 nK. The modulation amplitude ranged from 130 to 280 mG. The resonance frequency was determined by fitting the number of atoms lost as a function of frequency to a Lorentzian distribution. The shift in the resonance angular frequency with temperature was determined to be approximately linear, corresponding to about $0.6\,(k_B T/\hbar)$. Thus is close to our result $\frac{1}{2}\,(k_B T/\hbar)$ for the thermal shift in the angular frequency at which the harmonic association rate is maximum. Thompson et al. also measured the resonance frequency in Bose-Einstein condensates with a 50% condensate fraction. The resonance frequency was higher than that predicted from the mixture of a 0-temperature condensate and a thermal cloud.

Papp and Wieman used longitudinal modulation of the magnetic field to measure the binding energies of universal dimers in a mixture of ^{85}Rb and ^{87}Rb atoms [1, 3]. The scattering length was controlled using the Feshbach resonance at 265.4 G for ^{85}Rb atoms in the $|2, -2\rangle$ hyperfine state and ^{87}Rb atoms in the $|1, -1\rangle$ hyperfine state. The modulation amplitude ranged from 0.6 to 1.0 G. The resonance frequency was determined by fitting the number of atoms lost as a function of frequency to a Gaussian distribution. Their results for the binding energy of the dimer as a function of the bias magnetic field were consistent with the universal result proportional to $1/a^2$.

B. LENS Experiment

Weber, Barontini, Catani, Thalhammer, Inguscio, and Minardi, used longitudinal modulation of the magnetic field to measure the binding energies of dimers composed of ^{41}K and ^{87}Rb atoms [4]. The scattering length was controlled using the Feshbach resonances for ^{41}K atoms in the $|1, +1\rangle$ hyperfine state and ^{87}Rb atoms in the $|1, +1\rangle$ hyperfine state near 38.4 G and 78.7 G. The measurements were made on thermal gases of trapped atoms

with typical temperatures ranging from 200 to 600 nK. The typical modulation amplitude was 130 mG. The dimer binding energy was determined by fitting the number of atoms lost as a function of frequency to a model that they developed. The model involved nonlinear differential equations for three amplitudes associated with a ^{41}K atom, a ^{87}Rb atom, and a molecule. They observed dependence of the resonant modulation frequency on the modulation amplitude b that was approximately linear in b^2. They also observed subharmonic loss features. They used the first subharmonic loss feature to extend their measurements of the binding energy to higher frequency.

C. Innsbruck Experiment

Lange, Pilch, Prantner, Ferlaino, Engeser, Nägerl, Grimm, and Chin used longitudinal modulation of the magnetic field to measure the binding energies of dimers of ^{133}Cs atoms [5]. The scattering length was controlled using the Feshbach resonances at 48 G and 53 G for ^{133}Cs atoms in the $|3, +3\rangle$ hyperfine state. The measurements were made on thermal gases of trapped atoms with a typical temperature of 100 nK. The modulation amplitude typically ranged from 100 to 600 mG. The dimer binding energy was determined by fitting the number of atoms lost as a function of frequency to a Gaussian distribution. The measurements of the binding energy as a function of the bias magnetic field $\bar{B}$ were used to improve the determinations of the Feshbach resonance parameters.

D. Bar-Ilan Experiments

Gross, Shotan, Kokkelmans, and Khaykovich used longitudinal modulation of the magnetic field to measure the binding energies of dimers of ^{7}Li atoms in the $|1, +1\rangle$ hyperfine state [7]. The scattering length was controlled using the Feshbach resonance at 738.2 G. Gross, Shotan, Machtey, Kokkelmans, and Khaykovich used the same method to measure the binding energies of dimers of ^{7}Li atoms in the $|1, 0\rangle$ hyperfine state [8]. The scattering length was controlled using the Feshbach resonance at 893.7 G. The measurements were made on thermal gases of trapped atoms with a typical temperature of 1.5 μK. The modulation amplitude ranged from 150 mG to 750 mG. The dimer binding energy was determined by fitting the number of atoms lost as a function of frequency to the convolution of a Maxwell-Boltzmann distribution and a Gaussian distribution. The measurements of the binding energies as functions of $\bar{B}$ were used to improve the determinations of the Feshbach resonance parameters.

In a subsequent experiment, Machtey, Shotan, Gross and Khayokovich used longitudinal modulation of the magnetic field to observe the association of ^{7}Li atoms in the $|1, 0\rangle$ hyperfine state into Efimov trimers [9]. The measurements were made on thermal gases of trapped atoms with a typical temperature of 1.5 μK. The modulation amplitude ranged up to 1.6 G. The number of atoms remaining in the trap was measured as a function of the frequency of the oscillating magnetic field for different values of the bias magnetic field. There was a deep minimum in the remaining number of atoms at the dimer binding frequency. The association of atoms into the Efimov trimer was observed as a second less-pronounced minimum or as a shoulder in the loss feature associated with the dimer. The difference between the trimer and dimer binding energies was determined by fitting the number of atoms lost as a function of frequency to a double-peak Gaussian distribution.

E. Rice Experiment

Dyke, Pollack, and Hulet used longitudinal modulation of the magnetic field to measure the binding energies of dimers of ^{7}Li atoms [10]. The scattering length was controlled using the Feshbach resonance at $B_0 = 737.7$ G for ^{7}Li atoms in the $|1, +1\rangle$ hyperfine state. The other parameters in the expression for the scattering length in Eq. (2), as determined in Ref. [10], are $a_{\rm bg} = -20.0\, a_0$ and $\Delta = -174$ G. The measurements were carried out for both a Bose-Einstein condensate and a thermal gas of ^{7}Li atoms.

In the experiment on the BEC of ^{7}Li atoms in Ref. [10], they observed a narrow loss resonance as a function of the frequency, with the fraction of atoms remaining decreasing almost to 0. The dimer binding energy was determined by fitting the fraction of atoms lost as a function of the frequency to a Lorentzian distribution. Their results for the fraction of atoms remaining as a function of the frequency were shown for the bias magnetic field $\bar{B} = 734.5$ G. The fit gave the binding energy $h(450$ kHz), from which the scattering length was determined to be $\bar{a} \approx 1100\, a_0$.

In the experiment on the thermal gas of ^{7}Li atoms in Ref. [10], they observed broader loss resonances as functions of the frequency. Their results for the fraction of atoms remaining as a function of the frequency were shown for the bias magnetic field $\bar{B} = 734.5$ G and for three combinations of the amplitude b of the modulated magnetic field and the temperature T: (b, T)=$(0.57\,\mathrm{G}, 3\,\mu\mathrm{K})$, $(0.14\,\mathrm{G}, 3\,\mu\mathrm{K})$, and $(0.57\,\mathrm{G}, 10\,\mu\mathrm{K})$. The duration of modulation was in the range from 25 μs to 500 μs, but its value was not specified for each individual set (b, T). The number of atoms in the thermal clouds were also not specified in Ref. [10]. For each (b, T), there was a harmonic peak just above ω_D. A subharmonic peak just above $\frac{1}{2}\omega_D$ was evident only for (0.57 G, 3μK). For this (b, T), the minimum fractions remaining were about 0.3 in the harmonic loss feature and about 0.5 in the subharmonic loss feature. In Ref. [10], the dimer binding energy was determined by fitting the fraction of atoms lost to the convolution of a Lorentzian and a thermal Boltzmann distribution. In the fits to the harmonic loss features, the deviations of the minima from the dimer binding frequency were about $0.7\,(k_B T/\hbar)$ for both $(0.57\,\mathrm{G}, 3\,\mu\mathrm{K})$ and $(0.14\,\mathrm{G}, 3\,\mu\mathrm{K})$. Thus is close to our simple result $\frac{1}{2}\,(k_B T/\hbar)$ for the thermal shift in the angular frequency at which the harmonic association rate is maximum, which applies if $k_B T \ll \hbar\omega$. The deviation of the minimum from the dimer binding frequency was about $1.3\,(k_B T/\hbar)$ for $(0.57\,\mathrm{G}, 10\,\mu\mathrm{K})$. This is about 3 times larger than our simple result, but the temperature is too high for that simple result to be accurate. In the fit to the subharmonic loss feature, the deviation of the minima from half the dimer binding frequency is about $0.3\,(k_B T/\hbar)$ for $(0.57\,\mathrm{G}, 3\,\mu\mathrm{K})$. Thus is close to our simple result $\frac{1}{4}\,(k_B T/\hbar)$ for the thermal shift in the angular frequency at which the subharmonic association rate is maximum.

F. Association and Dissociation Rates

We use the conditions of the Rice experiment in Ref. [10] to illustrate our theoretical results on the association rates into dimers in a thermal gas of atoms. We also illustrate our results on the dissociation rates in a thermal gas of dimers. We consider ^{7}Li atoms in the $|1, +1\rangle$ hyperfine state at the bias magnetic field $\bar{B} = 734.5$ G, and we consider the same three combinations of the amplitude b of the modulated magnetic field and the temperature T: (b, T)=$(0.57\,\mathrm{G}, 3\,\mu\mathrm{K})$, $(0.14\,\mathrm{G}, 3\,\mu\mathrm{K})$, and $(0.57\,\mathrm{G}, 10\,\mu\mathrm{K})$.

In Fig. 1, we show our results for the association rates as functions of the angular frequency

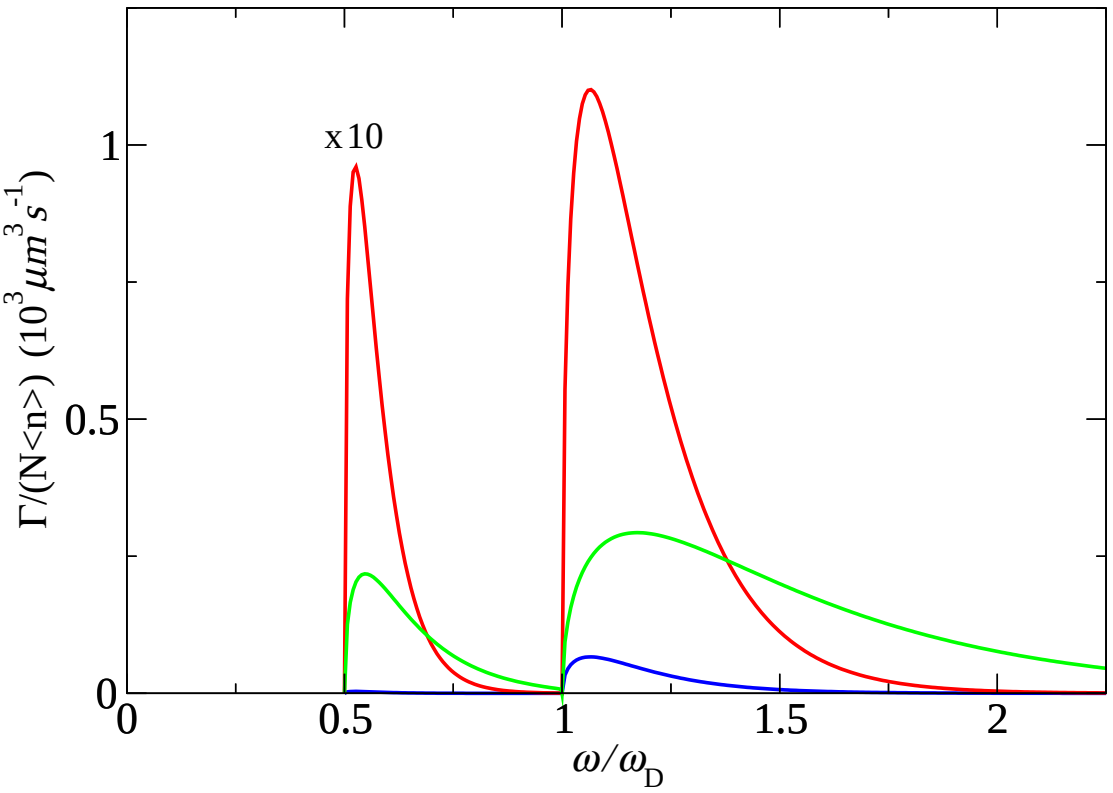

FIG. 1: Association rate $\Gamma/N\langle n\rangle$ for a thermal gas of ^{7}Li atoms as a function of the modulation frequency of the magnetic field. The angular frequency ω is normalized to the angular binding frequency ω_D of the dimer. The bias field is $\bar{B} = 734.5$ G, which corresponds to $\bar{a} \approx 1100\ a_0$. The three sets of curves are for different values of the modulation amplitude b and the temperature T: (b, T)=(0.57 G, 3 μK) (highest peak value, red), (0.57 G, 10 μK) (green), and (0.14 G, 3 μK) (lowest peak value, blue). The association rates in the region $\omega < \omega_D$ have been multiplied by 10 to make the subharmonic transitions more visible.

ω for the three sets of values of (b, T) for which the atom loss was measured in Ref. [10]. The ratio of $k_BT/\hbar$ to the binding frequency $\omega_D = \hbar/m\bar{a}^2$ of the dimer is 0.15 and 0.49 at the temperatures 3 μK and 10 μK, respectively. Thus the condition $k_BT \ll \hbar^2/m\bar{a}^2$ is much better satisfied at 3 μK. In Fig. 1, the curves for $\omega > \omega_D$ are the harmonic association rates $\Gamma_1^{(1)}(\omega)$ in Eq. (30) with $\int d^3r\, n_1 n_2$ replaced by $\int d^3r\, n^2/2$. The curves for $\omega < \omega_D$ are the subharmonic association rates $\Gamma_2^{(1,1)}(\omega)$ in Eq. (52) with $\int d^3r\, n_1 n_2$ replaced by $\int d^3r\, n^2/2$. The subharmonic association rates $\Gamma_2^{(2)}(\omega)$ are completely negligible: their peak values are smaller than those for $\Gamma_2^{(1,1)}$ by factors of about 3×10^{-5}. The association rates in Fig. 1 are divided by $\int d^3r\, n^2(\boldsymbol{r}) = N\langle n\rangle$ to obtain rates $\Gamma/N\langle n\rangle$ that do not depend on the number of atoms. The angular frequency is normalized to the angular binding frequency $\omega_D = \hbar/m\bar{a}^2$ of the dimer. The heights of the harmonic and subharmonic peaks for (b, T)=(0.57 G, 3 μK)

are larger than those for $(0.14\,\mathrm{G}, 3\,\mu\mathrm{K})$ by the ratio of the values of b^2, which is 12.8. The maxima of the harmonic association rates are at angular frequencies ω that are above the threshold ω_{D} by approximately $k_B T/2\hbar$. The maxima of the subharmonic association rates are at angular frequencies that are above the threshold $\frac{1}{2}\omega_{\mathrm{D}}$ by approximately $k_B T/4\hbar$. The ratios of the maximum of the harmonic peak to the maximum of the subharmonic peak are 11.4, 190, and 13.8 for (b, T)=$(0.57\,\mathrm{G}, 3\,\mu\mathrm{K})$, $(0.14\,\mathrm{G}, 3\,\mu\mathrm{K})$, and $(0.57\,\mathrm{G}, 10\,\mu\mathrm{K})$, respectively. They can be compared to the ratios 11.9, 198, and 24.1 predicted using Eq. (53).

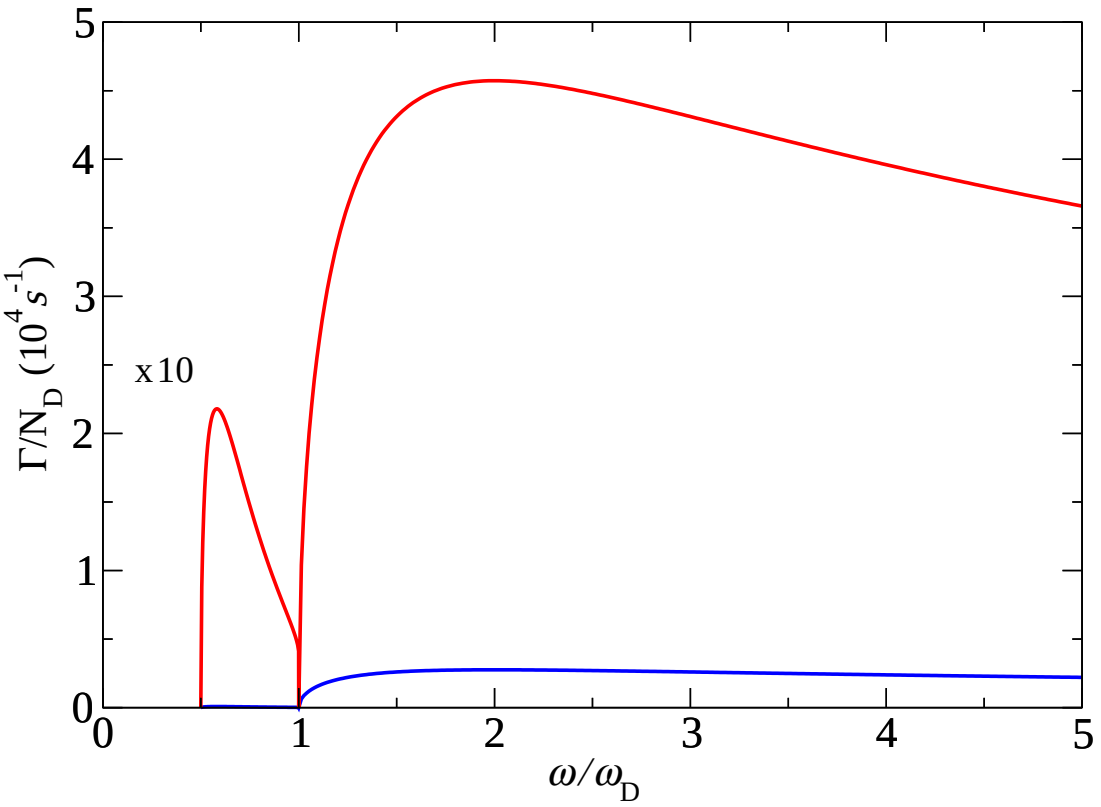

FIG. 2: Dissociation rate Γ/N_D for a thermal gas of ^{7}Li dimers as a function of the angular frequency ω of the modulated magnetic field. The angular frequency ω is normalized to the binding angular frequency ω_D of the dimer. The bias field is $\bar{B} = 734.5$ G, which corresponds to $\bar{a} \approx 1100\ a_0$. The dissociation rate is independent of the temperature. The two sets of curves are for different values of the modulation amplitude b: 0.57 G (higher peak value, red) and 0.14 G (lower peak value, blue). The dissociation rates in the region $\omega < \omega_D$ have been multiplied by 10 to make the subharmonic transitions more visible.

Our results for dissociation rates in a thermal gas of dimers as functions of the angular frequency ω are illustrated in Fig. 2 using the two values of b for which the atom loss was measured in Ref. [10]. The dissociation rates in Fig. 2 are divided by the number N_D of dimers to obtain rates Γ/N_D that do not depend on N_D. The angular frequency ω is normalized to the binding angular frequency ω_D of the dimer. The curves for $\omega > \omega_D$

are the harmonic dissociation rates $\Gamma_1^{(1)}(\omega)$ in Eq. (39). The curves for $\omega < \omega_D$ are the subharmonic dissociation rates $\Gamma_2^{(1,1)}(\omega)$ in Eq. (55). The subharmonic association rates $\Gamma_2^{(2)}(\omega)$ are completely negligible: their peak values are smaller than those for $\Gamma_2^{(1,1)}$ by factors of about 3×10^{-5}. The heights of the harmonic and subharmonic peaks for $b = 0.57$ G are larger than those for $b = 0.14$ G by the ratio of the values of b^2, which is 12.8. The maxima of the harmonic association rates are at twice the threshold angular frequency $\hbar/m\bar{a}^2$. For large ω, the harmonic rates decrease very slowly as $\omega^{-1/2}$. The maxima of the subharmonic dissociation rates are above the threshold angular frequency $\frac{1}{2}(\hbar/m\bar{a}^2)$ by only about 0.08 $\hbar/m\bar{a}^2$. The ratio of the maximum of the harmonic peak to the maximum of the subharmonic peak is given in Eq. (56). The ratios for $b = 0.57$ G and $b = 0.14$ G are approximately 21 and 340, respectively.

VIII. PREVIOUS THEORETICAL WORK

In this section, we describe previous theoretical treatments of the association of atoms into dimers using longitudinal modulation of the magnetic field by Hanna, Köhler, and Burnett [12], by Brouard and Plata [13], and by Bazak, Liverts, and Barnea [14].

A. Hanna, Köhler, and Burnett

A theoretical treatment of the association of atoms into dimers using longitudinal modulation of the magnetic field was first presented by Hanna, Köhler, and Burnett in 2007 [12]. They used a two-channel model for the two-atom system, with one channel consisting of a continuum of atom pairs labelled by the relative momentum vector $\boldsymbol{p}$ and a second channel consisting of a single discrete molecular state. The parameters of the model were not specified clearly. The eigenstate of the time-independent coupled-channel problem corresponding to the bias magnetic field $\bar{B}$ are a continuum of positive energy atom-pair states and a single discrete negative-energy state, which is the dimer. The parameters of the model were presumably chosen so that the dimer binding energy has its physical value, which can be approximated by $\hbar^2/m\bar{a}^2$. The time-dependent problem in Ref. [12] was obtained by adding $\mu b \sin(\omega t)$ to the energy of the discrete molecular state, where μ is the difference between the magnetic moments of the closed-channel molecule responsible for the Feshbach resonance and a pair of atoms in the open channel. They solved the time-dependent Schrödinger equation for the two-channel model numerically to obtain the probability for association of a pair of atoms with relative momentum p into the dimer as a function of time. They compared the results with first-order time-dependent perturbation theory in b. They calculated the conversion efficiency for atoms into dimers in a homogeneous gas by averaging the transition probabilities over a Gaussian thermal distribution of atom pairs. Hanna, Köhler, and Burnett also calculated the conversion efficiency in a Bose-Einstein condensate using a completely different method that involved solving numerically an integro-differential equation for the mean-field of a homogeneous BEC. Subharmonic transitions were not discussed in Ref. [12].

The results for the conversion efficiency in Ref. [12] are completely numerical. They calculated the conversion efficiency in a homogeneous gas as a function of the modulation time t, the modulation frequency ω, and the modulation amplitude b at several temperatures T.

They did not provide sufficient information to allow quantitative comparisons of the normalizations of their numerical results and our analytic results. They specified the magnetic field offset $\bar{B}$ and the dimer binding energy, but this is insufficient to determined the Feshbach resonance parameters $a_{\rm bg}$, B_0, and Δ that appear in our normalization factor. The only quantitative comparisons we can make are therefore of dimensionless ratios of conversion efficiencies. Their conversion efficiency initially increases approximately quadratically with t, but then increases a little less than linearly with t. Since we used Fermi's Golden Rule to derive our transition rates, the predicted increase in the conversion efficiency is strictly linear in t. Beyond the initial quadratic region of t, the ratios of their conversion efficiencies at three different temperatures agree with our analytic results to better than 10%. They calculated the conversion efficiency as a function of ω for four combinations of t and T. The ratios of the peak values of their conversion efficiencies agree with our analytic results to better than 10%. They also calculated the conversion efficiency as a function of b. It first increases approximately quadratically with b. It reaches a maximum, then decreases to near 0, and then increases to a second maximum. Since we used first order perturbation theory to derive our harmonic association rate, the predicted dependence on the conversion efficiency is strictly quadratic in b.

B. Brouard and Plata

Brouard and Plata have recently presented a different theoretical treatment of the association of atoms into dimers using longitudinal modulation of the magnetic field [13]. They described the two-atom system at the bias magnetic field $\bar{B}$ by a two-channel model, with one channel consisting of a continuum of atom pair states labelled by their energy E and the second channel consisting of a single discrete molecular state. The eigenstates of the time-independent coupled-channel problem are a continuum of positive-energy atom-pair states and a single discrete negative-energy state, whose binding energy $E_{\rm d}$ is that of the dimer. The time-dependent problem in Ref. [13] was obtained by adding $\mu b \sin(\omega t)$ to the energy of the discrete molecular state, as in Ref. [12]. However, rather than solving the time-dependent Schrödinger equation for their two-channel model, they reduced it to a two-state model consisting of the dimer and a single atom-pair state. They used a time-dependent unitary transformation to move all the time-dependence in the Hamiltonian into off-diagonal terms between the dimer state and the atom-pair state and change the dimer-dimer entry to $-E_{\rm d} + l\omega$, where l is an integer. They interpreted the time-average of the 2×2 Hamiltonian with $l = 1$ and with $l = 2$ as effective Hamiltonians that describe harmonic and subharmonic transitions, respectively. The entries of the effective Hamiltonian were given analytically as functions of ω, b, and the parameters of their time-independent two-state model. Brouard and Plata inferred some qualitative features of the association of atoms into dimers from these effective Hamiltonians.

In Ref. [13], Brouard and Plata also calculated the conversion efficiencies as functions of the modulation time and the frequency using a nonlinear equation for the amplitude of two coupled channels that represent the dimer and an atom pair. These results are all completely numerical.

C. Bazak, Liverts, and Barnea

The association rate of atoms into dimers using an oscillating magnetic field was calculated by Bazak, Liverts, and Barnea in 2012 [14]. They considered a time-dependent magnetic field $\boldsymbol{B}(t)$ that is the sum of the bias magnetic field $\bar{B}\hat{\boldsymbol{z}}$ and a small oscillatory term $b\sin(\omega t)$ from an electromagnetic wave with polarization in an arbitrary direction. The term in the Hamiltonian that involves the magnetic field is $-g\mu_{\rm B}\boldsymbol{S}\cdot\boldsymbol{B}(t)$, where $g\mu_{\rm B}\hbar/2$ is the magnetic moment of an electron and $\boldsymbol{S}$ is the spin of the valence electron of an alkali metal atom. They treated the time-dependent term from the oscillating magnetic field as a first-order perturbation. They used Fermi's Golden Rule to obtain an expression for the transition rate from a pair of atoms to a final state that consists of a dimer and an emitted photon. The transition matrix was simplified using the multipole expansion for the emitted photon. The leading terms are quadratic in the photon momentum, and consist of an s-wave term and a d-wave term. The matrix elements of the multipole operators between an atom-pair state and a dimer state were evaluated under the assumption that the atoms have a large scattering length and taking into account their effective range $r_{\rm eff}$.

Bazak, Liverts, and Barnea give an analytic result for the association rate into dimers [14]. Their result can be simplified by taking the limit $r_{\rm eff} \ll \bar{a}$. The factors that depend on the scattering length $\bar{a}$ and on the oscillation frequency ω are

$$\Gamma(\omega) \propto \frac{\kappa(\omega)}{\bar{a}^3}\left(1+\frac{16}{5}\frac{\hbar\bar{a}^2\kappa^4(\omega)}{m\omega}\right)\exp(-\beta\hbar^2\kappa^2(\omega)/m), \tag{57}$$

where $\kappa(\omega)$ is given by Eq. (31). The two terms inside the parenthesis are the s-wave and d-wave contributions, respectively. Near the harmonic threshold, the d-wave term is suppressed by a factor of $(\kappa\bar{a})^4$. Our harmonic transition rate $\Gamma_1^{(1)}$ in Eq. (30) has the same thermal factor $\exp(-\beta\hbar^2\kappa^2/m)$. The remaining dependence on ω is in the factor κ/ω. The remaining dependence on ω in Eq. (57) is in the factor κ in the s-wave term and in the factor κ^5/ω in the d-wave term. The different dependence on ω may be due to the assumption in Ref. [14] that the transition proceeds through the absorption of a real photon from an electromagnetic wave. In our derivation of the harmonic association rate, we assumed that the transition proceeds through the absorption of a quantum of energy from the oscillating magnetic field.

In Ref. [14], the prefactor of the expression on the right side of Eq. (57) is a product of many factors. Some of the factors are fundamental constants. There is a factor that depends on the direction and polarization of the electromagnetic wave and is maximal when the oscillating magnetic field is longitudinal. However there are other factors that are ill-defined. Those factors are the number of photons in the initial state with a specified momentum and polarization and a temperature-dependent factor that depends on an unphysical spherical confinement radius. Thus the normalization of the transition rate is not predicted in Ref. [14].

IX. SUMMARY

In this paper, we have further developed the new approach to transitions from longitudinal modulation of the magnetic field that was introduced in Ref. [15]. That approach was based on the realization that the leading effect of a longitudinal modulation of the magnetic field

near a Feshbach resonance can be treated as a time-dependent perturbation proportional to the contact operator C. In Appendix A, we presented a quantum field theory argument that the perturbation proportional to C can also be used beyond first order. Fermi's Golden Rule is used to obtain general expressions for transition rates in terms of transition matrix elements of C. Our general formula for the harmonic transition rate $\Gamma_1^{(1)}(\omega)$ in Eq. (8) comes from the first-order perturbation in C and was obtained previously in Ref. [15]. There is a contribution $\Gamma_2^{(2)}(\omega)$ to the subharmonic transition rate from the first-order perturbation in C that is related in a simple way to the harmonic rate and is given in Eq. (11). However the second-order perturbation in C gives another contribution $\Gamma_2^{(1,1)}(\omega)$ to the subharmonic transition rate that is given in Eq. (13). Near the Feshbach resonance, $\Gamma_2^{(1,1)}$ is larger than $\Gamma_2^{(2)}$ by a factor of $(\bar{a}/a_{\rm bg})^2$.

For a homogeneous system, our general expressions for the transition rates can be simplified by expressing the transition matrix elements of the contact operator C in terms of transition matrix elements of the contact density operator $\mathcal{C}$. The harmonic transition rate $\Gamma_1^{(1)}$ in Eq. (8) can be simplified by inserting Eq. (16). The subharmonic transition rate $\Gamma_2^{(1,1)}$ in Eq. (13) can be simplified by inserting Eq. (17). For a nonhomogeneous system in the local density approximation, these simplifications can first be used to calculate the transition rates for the homogeneous system. Substitutions such as those in Eqs. (18) and (19) can then be used to obtain the transitions rate for the nonhomogenous system.

To obtain association rates in a thermal gas of atoms and dissociation rates in a thermal gas of dimers, we first exploited the low density to reduce the transition matrix elements of $\mathcal{C}$ in the thermal gas to transition matrix elements of $\mathcal{C}$ in the two-body problem. Those matrix elements were calculated in Appendix B using the quantum field theory formulation of the problem of atoms with zero-range interactions. In the two-atom sector, this is equivalent to a single-channel model for atoms with large scattering length, with the dimer arising dynamically as a bound state. This allowed us to calculate the matrix elements of the contact density operator analytically.

Our final results for the harmonic and subharmonic association rates in a thermal gas of atoms are given in Eqs. (30) and (52). Our final results for the harmonic and subharmonic disssociation rates in a thermal gas of dimers are given in Eqs. (39) and (55). These results are analytic functions of all the relevant parameters: the oscillation parameters ω, b, and $\bar{a}$ or $\bar{B}$, the Feshbach resonance parameters $a_{\rm bg}$, B_0, and Δ, and the temperature T. The association rates in a thermal gas of fermions with two spin states depend on the local number densities $n_1(\boldsymbol{r})$ and $n_2(\boldsymbol{r})$ only through the multiplicative factor $\int d^3r\, n_1 n_2$. The dissociation rates in a thermal gas of dimers depend on the local number density $n_{\rm D}(\boldsymbol{r})$ only through the multiplicative factor $\int d^3r\, n_{\rm D}$. Our analytic results should be useful for analyzing experiments on association into dimers and dissociation of dimers. They should also be useful for designing experiments that optimize the number of dimers created or destroyed by the modulated magnetic field. For a thermal gas of atoms with $k_BT \ll \hbar^2/m\bar{a}^2$, the maximum in the harmonic association rate is at an angular frequency ω that is above the threshold $\hbar/m\bar{a}^2$ by approximately $\frac{1}{2}(k_BT/\hbar)$. The maximum in the subharmonic association rate is at an angular frequency that is above the threshold $\frac{1}{2}(\hbar/m\bar{a}^2)$ by approximately $\frac{1}{4}(k_BT/\hbar)$. For a thermal gas of dimers, the maximum in the harmonic dissociation rate is at an angular frequency ω that is approximately twice the threshold $\hbar/m\bar{a}^2$. The maximum in the subharmonic dissociation rate is at an angular frequency that is above the threshold $\frac{1}{2}(\hbar/m\bar{a}^2)$ by approximately $0.08\,(\hbar/m\bar{a}^2)$.

Our general results for the harmonic and subharmonic transition rates in terms of matrix elements of the contact density operator can also be applied to other systems. That reduces the problem to calculating transition matrix elements of the contact density operator between many-body states of the homogeneous system. An analytic result for the association rate in a dilute Bose-Einstein condensate of identical bosons was given in Ref. [15]. It should also be possible to obtain analytic results for superfluids of fermions with two spin states at zero temperature, including the dissociation rate of dimers in the BEC limit and the dissociation rate of Cooper pairs in the BCS limit. The dissociation rate of paired fermions in the unitary limit is more challenging, but it is an important problem because it would allow the first direct measurements of the gap for the unitary Fermi gas.

Acknowledgments

This research was supported in part by the National Science Foundation under grant PHY-1310862 and by the Simons Foundation. We thank Hudson Smith for valuable discussions.

Appendix A: Quantum Field Theory Derivation of Perturbing Hamiltonian

Particles with a scattering length a that is large compared to the range r_0 of their interactions can be described by a local quantum field theory. For a fermion with two spin states, there are two fermionic quantum fields ψ_1 and ψ_2. The interactions of the quantum field theory are made local by taking the zero-range limit at the expense of introducing an ultraviolet cutoff Λ on the momenta of virtual particles. The interaction Hamiltonian density is

$$\mathcal{H}_{\rm int} = (\lambda_0/m)\psi_1^\dagger\psi_2^\dagger\psi_2\psi_1, \tag{A1}$$

where λ_0 is the bare coupling constant. If $\hbar$ is set to 1, λ_0 has dimensions of length. The field theory describes particles with scattering length a if the bare coupling constant is

$$\lambda_0 = \frac{4\pi}{1/a - 2\Lambda/\pi}. \tag{A2}$$

Matrix elements of the operator $\psi_1^\dagger\psi_2^\dagger\psi_2\psi_1$ diverge as Λ^2 as the cutoff is increased to ∞. Since λ_0 scales as $1/\Lambda$, matrix elements of the interaction Hamiltonian density in Eq. (A1) therefore diverge as Λ. In matrix elements of the complete Hamiltonian density, the divergence is cancelled by a corresponding divergence in matrix elements of the kinetic energy density. In matrix elements of the operator $\psi_1^\dagger\psi_2^\dagger\psi_2\psi_1$, subleading terms that diverge as Λ give finite contributions to the energy density. The contact density operator in the quantum field theory is [18]

$$\mathcal{C} = \lambda_0^2\psi_1^\dagger\psi_2^\dagger\psi_2\psi_1. \tag{A3}$$

This operator has finite matrix elements, because the divergence in the matrix element of $\psi_1^\dagger\psi_2^\dagger\psi_2\psi_1$ proportional to Λ^2 is compensated by a factor of $1/\Lambda^2$ from λ_0^2.

The local quantum field theory can describe particles with a time-dependent scattering length $a(t)$ provided the time scale $a/\dot{a}$ is large compared to the time scale $mr_0^2/\hbar$ set by the range. In the interaction Hamiltonian density in Eq. (A1), the time-dependent bare coupling constant $\lambda_0(t)$ is obtained by replacing a in Eq. (A2) by $a(t)$. If the time dependence consists

of small deviations in the inverse scattering length from some value $1/\bar{a}$, the bare coupling constant can be expanded around the corresponding value $\bar{\lambda}_0$:

$$\lambda_0(t) = \bar{\lambda}_0 - \frac{\bar{\lambda}_0^2}{4\pi}\left(\frac{1}{a(t)} - \frac{1}{\bar{a}}\right) + \frac{\bar{\lambda}_0^3}{(4\pi)^2}\left(\frac{1}{a(t)} - \frac{1}{\bar{a}}\right)^2 + \dots. \tag{A4}$$

When this is inserted into the interaction Hamiltonian density in Eq. (A1), the term linear in $1/a(t)$ is proportional to the contact density operator in Eq. (A3). The term quadratic in $1/a(t)$ is suppressed by $1/\Lambda$ from the additional power of $\bar{\lambda}_0$. The higher order terms are even more highly suppressed. Thus the interaction Hamiltonian density in the zero-range limit can be reduced to

$$\mathcal{H}_{\rm int}(t) = \frac{\bar{\lambda}_0}{m}\psi_1^\dagger\psi_2^\dagger\psi_2\psi_1 - \frac{1}{4\pi m}\left(\frac{1}{a(t)} - \frac{1}{\bar{a}}\right)\mathcal{C}. \tag{A5}$$

Appendix B: Matrix Elements of the Contact density operator

The field theoretic definition of the contact density operator in Eq. (A3) can be expressed as

$$\mathcal{C}(\boldsymbol{r}) = \phi^\dagger(\boldsymbol{r})\phi(\boldsymbol{r}), \tag{B1}$$

where the *contact field* $\phi = \lambda_0\psi_2\psi_1$ is a local operator that annihilates two atoms at a point. In the case $a > 0$, $\phi(\boldsymbol{r})$ has a nonzero amplitude to annihilate a dimer, so it can also be referred to as the *dimer field*. The transition matrix element of the contact density operator can be expressed as

$$\langle f|\mathcal{C}(\boldsymbol{r})|i\rangle = \sum_n \langle f|\phi^\dagger(\boldsymbol{r})|n\rangle\langle n|\phi(\boldsymbol{r})|i\rangle. \tag{B2}$$

A complete set of states $\sum_n |n\rangle\langle n| = 1$ has been inserted between $\phi^\dagger$ and ϕ. If only one term in the sum is nonzero, the matrix element factors into a matrix element of ϕ that involves the initial state and a matrix element of $\phi^\dagger$ that involves the final state.

In order to calculate transition rates in a thermal gas of atoms or dimers, one needs to calculate transition matrix elements of the contact density operator $\mathcal{C}(\boldsymbol{r})$ between two-atom states, which are either a pair of unbound atoms or a dimer. We will calculate these matrix elements in the Zero-range Model defined by the interaction Hamiltonian density in Eq. (A1). The Feynman rules for the atom propagator and the 2-atom–to–2-atom vertex are specified in the appendix of Ref. [19]. The 2-atom–to–molecule coupling constant g_0 should be set to 0. Using these Feynman rules, the calculation of transition matrix elements of the contact density operator can be reduced to evaluating Feynman diagrams.

The transition amplitude $A(E_{cm})$ is the amplitude for the transition between a pair of atoms in the asymptotic past and a pair of atoms in the asymptotic future. It is a function only of the energy $E_{\rm cm}$ of the pair of atoms in their center-of-mass frame:

$$E_{\rm cm} = E - K^2/4m, \tag{B3}$$

where E is their total energy and $\boldsymbol{K}$ is their total momentum. (We set $\hbar = 1$ in this Appendix.) The transition amplitude can be calculated by solving the Lippmann-Schwinger equation shown in Figure 3:

$$iA(E_{\rm cm}) = -i(\lambda_0/m) + (\lambda_0/m)I(E_{\rm cm})A(E_{\rm cm}). \tag{B4}$$

The loop integral $I(E_{\rm cm})$ in the last diagram in Figure 3 is

$$I(E_{\rm cm}) = \frac{\lambda_0^2}{m} \int_{\boldsymbol{q}} \frac{1}{q^2 - mE_{\rm cm} - i\epsilon}, \tag{B5}$$

where $\boldsymbol{q}$ is the loop momentum. Using the expression for the bare coupling constant in Eq. (A2), the solution can be expressed as

$$A(E_{\rm cm}) = \frac{4\pi/m}{-1/a + \sqrt{-mE_{\rm cm} - i\epsilon}}. \tag{B6}$$

This amplitude has a pole in the energy at $E = K^2/4m - 1/ma^2$. The residue of the pole is $-Z_{\rm D}$, where

$$Z_{\rm D} = 8\pi/m^2 a. \tag{B7}$$

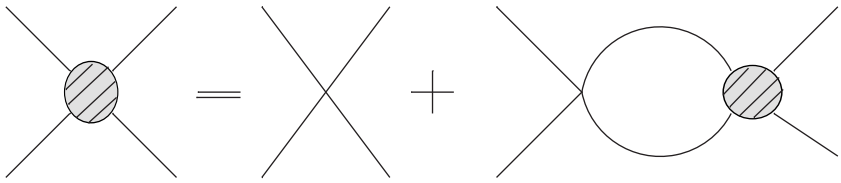

FIG. 3: The Lippmann-Schwinger equation for the transition amplitude $A(E_{\rm cm})$. The blob represents $iA(E_{\rm cm})$. The vertex factor is $-i\lambda_0/m$.

The standard Feynman rules can be used to calculate matrix elements of local operators between states in the asymptotic past and states in the asymptotic future. However we need matrix elements between initial and final states at the same time. We will use the Feynman rules to calculate matrix elements of the contact field operator $\phi^\dagger$ between the vacuum and two-atom states in the asymptotic future. We will then calculate matrix elements of the contact density operator $\phi^\dagger\phi$ between two-atom states in the asymptotic future by expressing them in terms of matrix elements of $\phi^\dagger$ and ϕ.

1. Vacuum-to-pair matrix element of $\phi^\dagger$

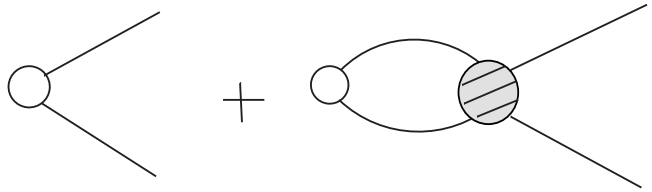

FIG. 4: Feynman diagrams for the matrix element of $\phi^\dagger(\mathbf{r})$ between the vacuum and the atom-pair state $|\boldsymbol{K}, \boldsymbol{k}\rangle$. The open dot represents the $\phi^\dagger$ operator, whose Feynman rule is λ_0. The residue of the pole in the energy in the second diagram can be used to determine the matrix element of $\phi^\dagger(\mathbf{r})$ between the vacuum and the dimer state $|\boldsymbol{k_D}\rangle$.

The matrix element of $\phi^\dagger(\boldsymbol{r})$ between the vacuum $|0\rangle$ and an atom-pair state $|\boldsymbol{K},\boldsymbol{k}\rangle$ with total momentum $\boldsymbol{K}$ and relative momentum $\boldsymbol{k}$ can be calculated from the Feynman diagrams in Fig. 4. The atoms are on their energy shells with total energy $E = K^2/4m + k^2/m$. The matrix element is

$$\begin{aligned}\langle \boldsymbol{K},\boldsymbol{k}|\phi^\dagger(\mathbf{r})|0\rangle &= \lambda_0\big[1 + iI(E_{\rm cm})A(E_{\rm cm})\big],\\ &= -mA(E_{\rm cm}).\end{aligned} \tag{B8}$$

The energy $E_{\rm cm}$ of the atom pair in their center-of-mass frame depends only on their relative momentum:

$$E_{\rm cm} = k^2/m. \tag{B9}$$

2. Vacuum-to-dimer matrix element of $\phi^\dagger$

The matrix element of $\phi^\dagger(\boldsymbol{r})$ between the vacuum $|0\rangle$ and a dimer state $|\boldsymbol{k}_{\rm D}\rangle$ with momentum $\boldsymbol{k}_{\rm D}$ can be calculated from second Feynman diagram in Fig. 4. That diagram has a pole in the total energy E of the final-state atoms, which must be off their energy shells. At the pole, the center-of-mass energy is equal to the binding energy of the dimer: $E_{\rm cm} = -1/ma^2$. The residue of the pole is the product of the desired matrix element and $Z_{\rm D}^{1/2}$, where $Z_{\rm D}$ is the residue factor given in Eq. (B7). The matrix element is therefore

$$\begin{aligned}\langle \boldsymbol{k}_{\rm D}|\phi^\dagger(\mathbf{r})|0\rangle &= i\lambda_0 I(E_{\rm cm})(-Z_{\rm D})Z_{\rm D}^{-1/2},\\ &= \sqrt{8\pi/a}.\end{aligned} \tag{B10}$$

3. Pair-to-pair matrix element of $\phi^\dagger\phi$

The matrix element of $\phi^\dagger\phi$ between the atom-pair states $|\boldsymbol{K},\boldsymbol{k}\rangle$ and $|\boldsymbol{K}',\boldsymbol{k}'\rangle$ in the asymptotic future can be calculated by inserting a complete set of states between $\phi^\dagger$ and ϕ, as in Eq. (B2) . Since the operator ϕ annihilates the initial-state atoms, the only term that contributes is the vacuum state. The matrix element factors into the vacuum–to–atom-pair matrix element and its complex conjugate:

$$\begin{aligned}\langle \boldsymbol{K}',\boldsymbol{k}'|\phi^\dagger(\mathbf{r})\phi(\mathbf{r})|\boldsymbol{K},\boldsymbol{k}\rangle &= \langle \boldsymbol{K}',\boldsymbol{k}'|\phi^\dagger(\mathbf{r})|0\rangle\langle 0|\phi^\dagger(\mathbf{r})|\boldsymbol{K},\boldsymbol{k}\rangle,\\ &= m^2 A^*(E_{\rm cm})A(E'_{\rm cm}),\end{aligned} \tag{B11}$$

where $E_{\rm cm}$ is given in Eq. (B3) and $E'_{\rm cm}$ is the same expression with k replace by k'.

The expression for this matrix element given in Ref. [19] is incorrect: the factor $A^*(E_{\rm cm})$ was not complex conjugated. It is easy to see that this is incorrect by setting the final state equal to the initial state: $\boldsymbol{K}' = \boldsymbol{K}$, $\boldsymbol{k}' = \boldsymbol{k}$. Since the operator is hermitian, the matrix element must be real. This condition is satisfied by Eq. (B11). The error made in Ref. [19] was that the matrix element was calculated not between atom-pair states at the same time, but between an atom-pair state in the asymptotic past and an atom-pair state in the asymptotic future.

4. Pair-to-dimer matrix element of $\phi^\dagger\phi$

The matrix element of $\phi^\dagger\phi$ between the atom-pair state $|\boldsymbol{K},\boldsymbol{k}\rangle$ in the asymptotic future and the dimer state $|\boldsymbol{k}_{\rm D}\rangle$ in the asymptotic future can be calculated by inserting a complete set of states between $\phi^\dagger$ and ϕ, as in Eq. (B2) . Since the operator ϕ annihilates the initial-state atoms, the only term that contributes is the vacuum state. The matrix element factors into a vacuum–to–dimer matrix element and the complex conjugate of a vacuum–to–atom-pair matrix element:

$$\begin{aligned}\langle \boldsymbol{k}_{\rm D}|\phi^\dagger(\boldsymbol{r})\phi(\boldsymbol{r})|\boldsymbol{K},\boldsymbol{k}\rangle &= \langle \boldsymbol{k}_{\rm D}|\phi^\dagger(\mathbf{r})|0\rangle\langle 0|\phi(\mathbf{r})|\boldsymbol{K},\boldsymbol{k}\rangle,\\ &= -m\sqrt{8\pi/a}\,A^*(E_{\rm cm}),\end{aligned} \tag{B12}$$

where $E_{\rm cm}$ is given by Eq. (B3).

5. Dimer-to-dimer matrix element of $\phi^\dagger\phi$

The matrix element of $\phi^\dagger\phi$ between the dimer states $|\boldsymbol{k}_{\rm D}\rangle$ and $|\boldsymbol{k}'_{\rm D}\rangle$ in the asymptotic future can be calculated by inserting a complete set of states between $\phi^\dagger$ and ϕ, as in Eq. (B2). Since the operator ϕ annihilates the initial-state dimer, the only term that contributes is the vacuum state. The matrix element factors into a vacuum–to–dimer matrix element and its complex conjugate:

$$\begin{aligned}\langle \boldsymbol{k}'_{\rm D}|\phi^\dagger(\boldsymbol{r})\phi(\boldsymbol{r})|\boldsymbol{k}_{\rm D}\rangle &= \langle \boldsymbol{k}'_{\rm D}|\phi^\dagger(\boldsymbol{r})|0\rangle\langle 0|\phi(\boldsymbol{r})|\boldsymbol{k}_{\rm D}\rangle,\\ &= 8\pi/a.\end{aligned} \tag{B13}$$

---

[1] S.T. Thompson, E. Hodby, and C.E. Wieman, "Ultracold molecule production via a resonant oscillating magnetic field," Phys. Rev. Lett. **95**, 190404 (2005) [cond-mat/0505567].

[2] M. Greiner, C.A. Regal, and D.S. Jin, "Probing the excitation spectrum of a Fermi gas in the BCS-BEC crossover regime," Phys. Rev. Lett. **94**, 070403 (2005) [cond-mat/0407381].

[3] S.B. Papp and C.E. Wieman, "Observation of heteronuclear Feshbach molecules from a ^{85}Rb–^{87}Rb gas," Phys. Rev. Lett. **97**, 180404 (2006) [cond-mat/0607667].

[4] C. Weber, G. Barontini, J. Catani, G. Thalhammer, M. Inguscio, and F. Minardi, "Association of ultracold double-species bosonic molecules," Phys. Rev. A **78**, 061601(R) (2008) [arXiv:0808.4077].

[5] A.D. Lange, K. Pilch, A. Prantner, F. Ferlaino, B. Engeser, H.-C. Nägerl, R. Grimm, and C. Chin, "Determination of atomic scattering lengths from measurements of molecular binding energies near Feshbach resonances," Phys. Rev. A **79**, 013622 (2009) [arXiv:0810.5503].

[6] S.E. Pollack, D. Dries, R.G. Hulet, K.M.F. Magalhaes, E.A.L. Henn, E.R.F. Ramos, M.A. Caracanhas, and V.S. Bagnato, "Collective excitation of a Bose-Einstein condensate by modulation of the atomic scattering length," Phys. Rev. A **82**, 020701(R) (2010) [arXiv:1004.2887].

[7] N. Gross, Z. Shotan, S. Kokkelmans, and L. Khaykovich, "Nuclear-Spin-Independent Short-Range Three-Body Physics in Ultracold Atoms," Phys. Rev. Lett. 105, 103203 (2010) [arXiv:1003.4891].

[8] N. Gross, Z. Shotan, O. Machtey, S. Kokkelmans, and L. Khaykovich, "Study of Efimov physics in two nuclear-spin sublevels of ^{7}Li," Comptes Rendus Physique **12**, 4 (2011) [arXiv:1009.0926].

[9] O. Machtey, Z. Shotan, N. Gross, and L. Khaykovich, "Association of Efimov trimers from a three-atom continuum," Phys. Rev. Lett. **108**, 210406 (2012) [arXiv:1201.2396].

[10] P. Dyke, S.E. Pollack, and R.G. Hulet, "Finite range corrections near a Feshbach resonance and their role in the Efimov effect," Phys. Rev. A **88**, 023625 (2013) [arXiv:1302.0281].

[11] D.H. Smith, "Inducing resonant interactions in ultracold atoms with a modulated magnetic field," arXiv:1503.02688.

[12] T.M. Hanna, T. Koehler, and K. Burnett, "Association of molecules using a resonantly modulated magnetic field," Phys. Rev. A **75**, 013606 (2007) [arXiv:cond-mat/0609725].

[13] S. Brouard and J. Plata, "Feshbach molecule formation through an oscillating magnetic field: subharmonic resonances," J. Phys. B: At. Mol. Opt. Phys. **48**, 065002 (2015) [arXiv:1503.01700].

[14] B. Bazak, E. Liverts, and N. Barnea, "Multipole analysis of radio-frequency reactions in ultracold atoms," Phys. Rev. Lett. **86**, 043611 (2012) [arXiv:1207.5936].

[15] C. Langmack, D.H. Smith, and E. Braaten, "Association of atoms into universal dimers using an oscillating magnetic field," Phys. Rev. Lett. **114**, 103002 (2015) [arXiv:1406.7313].

[16] S. Tan, "Large momentum part of fermions with large scattering length," Ann. Phys. **323**, 2971 (2008) [cond-mat/0508320].

[17] E. Braaten and H. -W. Hammer, "Universal relation for the inelastic two-body loss rate," J. Phys. B **46**, 215203 (2013) [arXiv:1302.5617].

[18] E. Braaten and L. Platter, "Exact relations for a strongly-interacting Fermi gas from the operator product expansion," Phys. Rev. Lett. **100**, 205301 (2008) [arXiv:0803.1125].

[19] E. Braaten, D. Kang, L. Platter, "Exact relations for a strongly-interacting Fermi gas near Feshbach Resonance," Phys. Rev. A. **78**, 053606 (2008) [arXiv:0806.2277].